Accuracy of commercially available implant planning softwares

by

Shamsher Sandlas

B.Sc., The University of British Columbia, 2010

D.M.D, The University of British Columbia, 2015

A THESIS SUBMITTED IN PARTIAL FULFILLMENT OF

THE REQUIREMENTS FOR THE DEGREE OF

MASTER OF SCIENCE

in

THE FACULTY OF GRADUATE AND POSTDOCTORAL STUDIES

(Craniofacial Science)

THE UNIVERSITY OF BRITISH COLUMBIA

(Vancouver)

May 2021

The following individuals certify that they have read, and recommend to the Faculty of Graduate and Postdoctoral Studies for acceptance, the thesis entitled:

Accuracy of commercially available implant planning softwares

submitted by Shamsher Sandlas in partial fulfillment of the requirements for

the degree of Master of Science

in Craniofacial Science

Examining Committee:

Dr. David MacDonald – Professor, Department of Oral Biological and Medical Sciences, UBC
Supervisor

Dr. Flavia Lakschevitz – Clinical Associate Professor, School of Dentistry, University of Minnesota
Supervisory Committee Member

Dr. Babak Chehroudi – Clinical Professor, Department of Oral Health Sciences, UBC
Supervisory Committee Member

Dr. Vincent Lee – Assistant Professor of Teaching, Department of Oral Health Sciences, UBC
Additional Examiner

Additional Supervisory Committee Member:

Dr. David Kennedy – Clinical Professor, Department of Oral Health Sciences, UBC
Supervisory Committee Member

Abstract

Objectives: Cone-Beam Computed Tomography (CBCT) was first developed 29 years ago and came into commercial use in 1999 and has over the last decade been increasingly applied to almost every area of dental practice. This is due to 3D visualization of teeth and supporting tissues, high spatial resolution, low radiation, and minimal operating time compared to medical computed tomography. The CBCT images are read by an accompanying viewer or a treatment planning software. Currently, there is little information on comparing accuracy of commercially available implant planning softwares. Therefore, the aim of this study was to assess the accuracy of four popular implant planning software (coDiagnostix, DTX, Simplant, and BlueSkyPlan) by identifying the mandibular canal using the free hand nerve marking tool.

Methods: Two De-fleshed human mandibles were acquired for study. Various regions of the mandibles were evaluated including canine, premolars, and molars. Gutta-percha was fixated in buccal and lingual aspects of the aforementioned regions. Mandibles were scanned in low (.30mm voxel size) and high (.18mm voxel size) resolution along with variation of mA values including 3.2, 4, and 5. DICOM files were imported into the four implant planning softwares for analysis. After image analysis, specimen were sectioned with a reverse-cutting saw in all evaluated regions. For gold standard measurements, a digital caliper was used in anatomical sections to measure comparable areas.

Results: ANOVA analysis demonstrated that there is no statistical significance between the gold standard and different softwares when calculating for accuracy. When calculating for sensitivity, it appears that coDiagnostix has the highest value out of the four softwares.

Conclusions: Varying mA and voxel size values does not impact the accuracy of four different softwares. It appears that coDiagnostix has the highest sensitivity values when using the most common settings for CBCT image acquisition.

Lay Summary

CBCT was first developed 29 years ago and came into commercial use in 1999 and has over the last decade been increasing applied to almost every area of dental practice. This is due to its better spatial resolution(image detail), lower radiation dose and smaller foot print and lesser operating requirements than medical computed tomography. Once a CBCT is taken, the data is saved or converted into a DICOM file. A software is needed to view these files. We compared the accuracy three commercially available implant planning softwares along with freeware software that is readily available by using mandibular canal as a landmark along with other regions of interest. We also tested whether changing CBCT scanning parameters would affect the accuracy of either of these softwares. The results demonstrated that no clinically significant difference is noted among the softwares and changing CBCT parameters did not affect the accuracy.

Preface

I conducted this in-vitro clinical study under the indispensable guidance of my supervisor Dr. David MacDonald and my committee members Dr. Flavia Lakschetivz and Dr. Babak Chehroudi.

I was responsible for collecting the data. The methodology was reviewed and planned under the guidance of Dr. Flavia Lakschetivz. Human mandibles for the study were provided by the UBC Anatomical Committee at Department of Cellular and Physiological Sciences. All of the scans and sectioning of the mandibles were conducted by me. I also conducted all the measurements in the softwares and caliper readings.

Ms. Sherry Gao from the statistics department along with Dr. Flavia Lakschevitz and Dr. Babak Chehroudi helped me immensely with the statistical analysis.

Ethics approval certificates were granted for all parts of this study from UBC Clinic Research Ethics Board (Certificate number: H19-02646)

Table of Contents

List of Tables

List of Figures

Glossary

2D – Two dimensional

3D – Three dimensional

ALARA – As Low As Reasonably Achievable

ANOVA – Analysis of Variance

BSP – Blue Sky Plan

CBCT – Cone Bean Computed Tomography

COVID-19 – Coronavirus Disease

coD – CoDiagnostix

CT – Computed Tomorgraphy

DHCP – Dental Health Care Practitioners

DICOM - Digital Imaging and Communications in Medicine

DPR – Dental Panoramic Radiograph

DTX – DTX Studio Implant

FOV – Field of View

I – Right Incisor

IAN – inferior alveolar nerve

kVp – Peak Voltage

LC – Left Canine

LP1 – Left First Premolar

LP2 – Left Second Premolar

LM1 – Left First Molar

LM2 – Left Second Molar

mA – Milliamperage

mm - Millimeter

MRI – Magnetic Resonance Imaging

PPE – Personal Protective Equipment

RC – Right Canine

RP1 – Right First Premolar

RP2 – Right Second Premolar

RM1 – Right First Molar

RM2 – Right Second Molar

SCT – Spiral Computed Tomograph

SM - Simplant

Acknowledgments

First, I would like to thank Dr. David MacDonald for not only helping me immensely by being my project supervisor but also being a great mentor throughout this entire process. It has been a pleasure to work with him. Throughout this process, we faced the common challenges and difficulties as many residents have throughout their graduate endeavors however the COVID-19 pandemic amplified many of those challenges. Dr. David MacDonald was extremely helpful in receiving access to continue the project as to maintain the proper timeline. His feedback was thorough and helped me grow as a researcher and a clinician. I will always to be grateful to have Dr. MacDonald guide me through this journey.

I would also like to extend my gratitude to my committee members, Dr. Flavia Lakschevitz and Dr. Babak Chehroudi. Dr. Laskchetivz was instrumental in helping establish the methodology in this study. She also helped me immensely in setting up the data analysis for this study. More than just logistics, she was always there to be a sounding board for suggestions and feedback for the project. I will always be grateful to her for always being there to respond to my concerns quickly and efficiently. Furthermore, she was program director for my first two years in the program and made her available to a great extent to ensure I was making the most out of my clinical studies. I also want to thank Dr. Chehroudi for making himself available throughout this process. His feedback on the project and contributions to data analysis were instrumental for us to reach the finish line. His input was extremely thorough and thoughtful, and his expertise was greatly appreciated.

I would also like to acknowledge Ms. Sherry Gao from the statistics department who helped me greatly in establishing the accuracy models and data analysis for this project. She was thorough, detailed and a pleasure to work with.

I would like to thank Mr. Aryan Johal for aiding me in sectioning of the mandibles. His expertise of power tools and equipment were invaluable and helped play a tremendous role in this project.

Lastly, I would like to extend my gratitude and great deal of appreciation to Grad Perio faculty and staff and of course my fellow co-residents. I want to thank my clinical instructors for spending valuable time to educate and mentor me. Their guidance and words of wisdom will never be forgotten. To my co-residents who have become a second family. As with any family, we have had tremendous ups and downs but throughout all of it we have managed to stay together and created lifelong relationships. I want to thank you for from the bottom of my heart for supporting me throughout this journey and I will always cherish the time we have spent together.

Dedication

This is detected to my parents, Jagjit and Narinder Sandlas. When I was young, I was told I could not “do” a lot of things but never once was I told that I couldn’t achieve anything. They believed in me to do things in which, only I could make possible. With such overwhelming belief, success and achievement are not a question of “if” but “when”. I want to thank them from the bottom of my heart. My life and successes stand upon their shoulders. Their guidance has led to me to pursue things with passion and instilled in me to excel in all ventures of life.

Chapter 1: Introduction to imaging in periodontics

Many options exist for radiographic imaging to properly diagnose and treatment plan patients undertaking periodontal treatment including dental implants. These options include standard modalities such as periapical radiographs, bitewing, occlusal radiographs, and panoramic images (Carranza, pg. 1054). Some of the more multidimensional modalities include conventional x-ray tomography, computed tomography (CT), and the cone-beam CT (CBCT) (Carranza 11e, page 1054).

1.1 Two – dimensional Imaging in Periodontics

Periapical radiographs provide a great advantage for assessment of the dentition and the edentulous site. There are relatively inexpensive and can be easily accessible in nearly all dental clinics in North America. In addition, they generate relatively low radiation to the patient (MacDonald, 2020 page 93). One of the biggest disadvantages as noted by Sewerin (1990) is their vulnerability to unknown magnification (foreshortening or elongation) of anatomical structures. This can result in poor reliability and inaccurate measurements. In addition, they are two dimensional images thereby limiting the amount of information that can be ascertained from a bucco-lingual direction (Carranza 11e, page 1055). Furthermore, the extent of the images may be limited by the size of the film (Carranza 11e, page 1055).

Occlusal radiographs are another modality that can be utilized. Similar to periapical radiographs, they provide an low-cost, low-radiation option to the clinician. In contrast to periapical film, occlusal radiographs can information in the buccal-lingual direction (White and Pharoah 6e, Page 147) Furthermore, they may be able to provide more information in a cross-sectional dimension as they cover a greater surface area than the periapical film (White and

Pharoah 6e, Page147). Similar to periapical film, occlusal radiographs face similar challenge in that they are prone to distortions (Carranza 11e, page 1055).

To avoid distortions such as foreshortening or elongation, parallel technique is recommended to ensure as much accuracy of the image as possible (White and Pharoah 6e, page 135). One of most common radiographs used in clinical dentistry is the bite-wing radiograph. It is taken when teeth are set in occlusion (White and Pharaoh 6e, page 135). One of the biggest advantages of the bite-wing radiograph over the periapical or occlusal is that it offers much less distortions (White and Pharoah 6e, page 135) and offers a great technique to acquire information regarding lesions in the proximity of the crown of the tooth such as cavitation. However, similar to periapical radiographs is that it doesn't offer information in a buccal-lingual direction. Furthermore, it is limited as it does not provide information in the apico-coronal extent as the periapical and may limit the amount of information that can be ascertained to certain landmarks such as inferior alveolar nerve and maxillary sinus.

One of the most common extra-oral imaging in clinical dentistry is the panoramic radiograph. Some of the advantages of the panoramic radiograph include, assessment of greater area of the intra-oral cavity and surrounding structures which allows for evaluation of important anatomical structures including the inferior alveolar canal and maxillary sinus (Carranza 11e, page 1056). In addition, it allows for the evaluation of extensive edentulous site and surrounding structures. Furthermore, it also offers relatively low dose radiation to the patient as compared to conventional three dimensional imaging (White and Pharoah 6e, page 248). Similar to intra-oral imaging discussed before, it only provides a two dimensional image. It is also prone to distortions in both the horizontal and vertical dimensions (Carranza 11e, page 1056). In addition, due to parameters and the angulation of the patient relative to the machine, there can be ghost

images, superimpositions, and variable horizontal and vertical magnifications (Carranza 11e, page 1056). Such conditions can cause inaccurate measurements. For these reasons, although the panoramic radiograph can provide a general broad image of the both the maxillary and mandibular arch, it does not provide a greater degree of detailed imaging as compared to intra-oral imaging (Carranza 11e, page 1056).

1.1.1 Imaging and COVID

It is also prudent to highlight how imaging and the prescription of radiographs may be affected during the period of the COVID-19 pandemic. Proper PPE is an essential to avoid the acquisition and transmission of the virus. During the pandemic, it is crucial to avoid generating aerosols to lower the spread of the virus as much as possible. It is important to consider that aerosols can be produced during intraoral radiographs (MacDonald et al. 2021). Studies have noted that the incidence rate of gagging during intraoral radiographs is 9% and 26% for trained radiographers and students, respectively (Sewerin 1984, MacDonald et al. 2021). Such incidence rates are astounding to any clinician as intraoral radiographs are widely used in day to day clinical practice. Furthermore, due to the extensively used CCD for intra-oral radiographs, the equipment itself presents a challenge as it cannot be sterilized (MacDonald et al. 2021). Dave et al. (2020) have recommended that two DHCP (dental health care workers) would be necessary to take intraoral radiographs. This would require extra staff resources and the necessary PPE to follow protocol which would present tremendous challenge to any dental clinic. It is therefore imperative to note that it may be in the best overall safety of the patient and the DHCP to use alternative methods of radiographs such as digital panoramic radiograph (DPR) and CBCT where possible. DPR has shown to be equally affective in the diagnosis of caries when combined with selective periapicals (Akkaya et al. 2006, MacDonald et al. 2021). Furthermore, DPR may

also reduce the propensity for the gag reflux during imaging (Farman 2002). CBCT has been shown to demonstrate distinct advantages especially as it pertains to endodontic diagnosis and treatment planning, evaluation of oral lesions and pathologies and implant planning (MacDonald et al. 2021). While DPR and CBCT may provide an alternative, both modalities do generate higher radiation dose to the patient (MacDonald et al. 2021). It is therefore imperative that we understand the limitations of such technologies and a decision should be made thoroughly evaluating the presenting clinical condition of the patient and the health risk as it relates to COVID-19 (MacDonald et al. 2021).

1.2 Three – Dimensional imaging in periodontics

Since it's first introduction into dentistry in the 1990's, cone beam CT (CBCT) has become a widely used imaging modality in periodontics and more specifically implant dentistry (Carranza 11e, page 1058, Arai et. al 1999). CBCT in an imaging modality which uses a conical shaped beam of x-ray photons to generate a 3D image (MacDonald, 2020). The hardware of a CBCT machine involves X-ray tube, internal and external filtration, fixated C-arm to allow for rotation in horizontal plane, and X-ray detector (Pauwels et al. 2015). Image is acquired as the x-ray tube is rotated in a circular motion (Pauwels et al. 2015). As the rotation occurs, the x-rays from the beam result in numerous two-dimensional projections which are captured by the detector. These projections or images are used to reconstruct a three-dimensional portrayal of the object (Pauwels et al. 2015).

While the use of CBCT has been noted, the variables and their set parameters are not yet a universal standard (Pauwels et al. 2015). It is important to understand that the CBCT rendered image is dependent upon many variables including mA, kVp, FOV, voxel size, and rotation arc (Pauwels et al. 2015). Effecting one or many of the variables can have an impact on the image

quality and radiation dose that is affecting the patient. Studies regarding these variables have been done to ensure an adequate image for clinical diagnosis can be achieved while maintaining the ALARA principle.

The advantages of CBCT to conventional dental radiography is that it is able to generate both a 3D and a 2D image (MacDonald, 2020). Furthermore, it's advantages over conventional 3D imaging such as Spiral Computed Tomography (SCT) in that the CBCT allows for better spatial resolution. This is attributed to SCT having anisotropic cuberilles whereas CBCT has isotropic cuberilles (MacDonald, 2020 page 78). In addition, the CBCT renders a 3D rendition by generating the cuberilles directly. Furthermore, the cost of CBCT is much less than a SCT and MRI in addition to less radiation dose than the HCT (MacDonald, 2020). While it's able to generate an image that is sufficient for hard-tissue it cannot capture and portray soft tissue as well as the MRI machine. This is of minimal concern as most of implant planning involves bone volume, density, and proximity to important landmarks such as the mandibular canal. It is also important to note that the AAP advocates the use of CBCT in implant planning to assess the location of important anatomical structures and communication for fabrication of surgical guides and restorative colleagues (Mandelaris et al. 2017).

1.3 Important mandibular anatomical landmarks in implant dentistry

Having good knowledge of head and neck anatomy is vital for implant dentistry because the process of implant placement entails a surgical phase and therefore from the incision to final suture, many landmarks and vital structures are part of the continuum to yield an optimal surgical result. For implants placement, the clinician must understand the hard tissue and components of the soft tissue such as blood vessels and nerves to avoid any complications. Complications can

occur in the form of infection, hemorrhage, nerve damage and perhaps even potentially fatal sequelae such as airway impingement. For implant placement, important landmarks to note can be divided into the maxilla and mandible. For the mandible, important landmarks and structures include mandibular canal (inferior alveolar nerve), lingual nerve, mental foramen and nerve, and the blood vessels in the anterior mandible.

Lingual nerve is a very important nerve and any damage which may result in paresthesia or dysesthesia can affect a person's quality of life. The lingual nerve provides sensory innervation to the anterior two/thirds of tongue and lingual tissues. Chan et al. (2010) states the location of the lingual nerve is located approximately 2mm lateral to the lingual plate and 3mm inferior to the crestal bone height in the area of third molar. The authors in the study observed that in approximately 42% of cases, the nerve coursed medially in direction of the tongue in the area of first molar. This was also seen in approximately a third and a quarter of the time in the area of second molar and premolar respectively. Furthermore, the authors observed that the nerve coursed medially away from the lingual cortex at approximately 58% and 17% in the area of first molar and second premolar respectively. Interestingly, the authors also detected that in one of the subjects, its course was changed in the first premolar region. It must be noted that these measurements were derived using two methods, taking an actual measurement from cadaver dissection and using linear measurement from CBCT with an adjunct use of a wire in the canal space.

Other structures of great significance in the mandible include the mental foramen and subsequently the mental nerve. Mental nerve is a continuation of the inferior alveolar nerve (IAN) as it navigates from the lingual aspect of the mandible to buccal aspect of the mandible moving anteriorly. As it crosses over to the buccal aspect, it travels through the mental foramen.

It was demonstrated that the foramen was situated approximately 28 mm from the mandible's midline and approximately 15 mm away from the mandible's inferior border (Greenstein and Tarnow 2006, Agthong et al. 2005). Neiva et al. (2004) found similar observations from direct measurements and reported the foramen was on average 27.6 mm from the midline and approximately 12mm from the inferior aspect of the mandible's cortex. Fishel et al. (1976) reported the incidence of mental foramen's location in the vertical plane for the first and second pre-molar using convention periapical radiographs. The authors noted an incidence of approximately 53% and 39% when the foramen was at the apex of or coronal to the second and first bicuspid respectively. This of great significance and one the clinician needs to be aware if planning on doing any sort of surgical procedures in the area.

While this was significant at the time, further studies demonstrated the disadvantages of using conventional radiographs. Phillips et al. (1990) observed the incidence of mental foramen to be only 75% when studying periapical radiographs. Furthermore, Yosue and Brooks (1989) observed the appearance of mental foramen on periapical and panoramic radiographs. The authors determined that panoramic and periapical films were less than 50% accurate in verifying the position of the mental foramen when comparing to its anatomical position. Further discrepancy of linear measurement errors at the mental foramen was demonstrated by Sonick et al. (1997). The authors observed measurement errors in range of 24% and 14% for panoramic and periapical radiographs, respectively. In their study, CT scans had fewest incidence of errors at 1.8%.

The inferior alveolar nerve (IAN) courses the mandible anteriorly to give rise to the mental nerve through the mental foramen. IAN is associated with hard tissue landmark, the mandibular canal which contains the IAN. IAN is a branch of the trigeminal nerve and

transverses through the mandibular canal. The IAN provides sensory innervation to the mandibular teeth including the buccal gingiva of mandibular teeth, sensation to the lower lip and including muscles of soft palate (Morton et al. 2019). In addition to housing the IAN, the mandibular canal also houses the inferior alveolar artery which supplies vascularity to the mandibular teeth. The complications associated with surgical intervention resulting in trauma in the area via extractions, implants and/or soft and hard tissue augmentation include intra-operative hemorrhage, pain, swelling and post-operative neurological complications such as dysthesia, paresthesia which can be permanent. The incidence rate of complications due to such procedures can be as high as 8.4% (Doh et al. 2018).

The course of the IAN may be present in various configurations. The nerve proceeds in downward fashion from the ramus and runs anterio-medially from the proximity of the mandibular ramus towards the mental foramen (Greenstein and Tarnow 2006, Morton et al. 2019). The nerve crosses the midsection from the lingual to the buccal aspect in the proximity of the first molar (Greenstein and Tarnow 2006). The average distance of the mandibular canal to the apices of dentate teeth was observed by Denio et al. (1992) in 22 dry human mandibles. The authors noted the average distance from the apices to the mandibular canal to be 4.7, 6.9 and 3.7mm in premolars, first and second molar respectively. Denio el al. (1992) also observed that by using conventional radiographs (periapical film), in approximately 28% of the cases mandibular canal could be visibly recognized in the second premolar and first molar area. Besides a periapical film, imaging modality to view the mandibular canal would include conventional and digital panoramic image, CBCT, and a multislice CT.

Greennow and Tarnow (2006) have provided safety guidelines to prevent mental nerve injury from surgical interventions such as dental implants. They recommend keeping a “safety

zone". The ‘‘safety zone’’ takes into account that the most superior part of the mental foramen is situated approximately 2 mm superior to the mandibular canal or IAN. Either in the presence or absence of anterior loop, Greenstein and Tarnow (2006) suggest that implant should be placed in a position where it's most posterior aspect is kept at distance greater than 2mm from the mental foramen to provide adequate space for surgical error without the risk of injury to the nerve.

1.4 Accuracy of CBCT in identifying mandibular canal and relevant mandibular anatomy

The accuracy of CBCT is dependent on numerous factors. There are many studies to showcase a higher accuracy of CBCT than conventional radiographs such as DPR or periapical films as highlighted before. It must be pointed out that accuracy pertaining to landmarks such as lingual nerve and IAN have been studied extensively. The study conducted by Chan et al. (2010) determined the mean difference between clinical detection of lingual nerve and CBCT data was 0.57mm however it had a standard deviation of 2.62mm which is well above the safe zone for implant placement noted by Greenstein and Tarnow (2006). These authors noted that such a large deviation could be due to the head positioning of the cadaver and movement of the nerve during dissection resulting in inaccurate clinical readings. While it's important to note that mean data may be quite minimal such as half of millimeter, it is clinical significance is substantial as it can dramatically impact clinical and patient outcomes.

There have been studies to note that CBCT is even helpful to the less experienced clinician. Radic et al. (2018) observed that the diagnostic accuracy of detecting lesions was significantly higher among residents when they were using the CBCT to evaluate the lesion. Furthermore, nearly all of the residents in the study noted that the dental panaromic radiograph (DPR) image did not provide sufficient information.

Naitoh el a. (2010) compared the CBCT to multisliced CT for identifying and detecting mandibular structures including the mandibular canal and the bifurcation of it along with accessory canal and formina. Both imaging modalities were able to find the bifid mandibular canals along with other mandibular structures. The authors observed that there was no significant difference between either modality in identifying and depicting these structures. It is important to note that for this study both imaging data were exported as DICOM file and viewed on the same software. The study noted that CBCT provides clear advantages over the MSCT via reduced radiation dose and providing a higher resolution.

Angelopolous et al. (2008) carried out a comparison study to evaluate the identification of the mandibular canal by using direct panoramic image, digital panoramic image and a CBCT generated image. The mandible was divided into three segments: posterior, middle and anterior and the images were rated based on the visibility of the mandibular canal. In all instances, the CBCT images were deemed to be of higher quality to both panoramic images in all instances. However, the authors do caution that CBCT should not replace digital panoramic images due to the concern with higher radiation.

Similarly, Jung and Cho (2014) evaluated the course and visibility of the mandibular canal by using DPR and CBCT generated images. The authors evaluated the visibility of the canal from the first to the third molar region. The results demonstrated that the visibility of the mandibular canal was far poor in panoramic images where it was deemed not visible in 22.7%, 11.8%, and 1.3% in the first, second, and third molar region respectively. In comparison, the CBCT images these values were 8.2%, 5.7% and 0.2% in their corresponding regions. The authors concluded that the CBCT provided a better visibility of the mandibular canal in the regions for first, second, and third molars than the panoramic radiographs.

Systematic review by Fokas et al. (2018) reviewed various publications as it related to the accuracy of CBCT in assessing linear measurements. The overall results indicate that CBCT provides a higher accuracy and reliability for hard tissue measurements and on images concerned with implant planning. They also note that wide range of inaccuracy when conducting linear measurements still remain with both overestimation and underestimation of the gold standard. These authors also note that there is a wide range of parameters resulting in varying mA, kvP, and voxel size which are not standardized. Furthermore, the accuracy of these measurements is always interpreted through an imaging software which are as variable as the CBCT machine (Fokas et al. 2018). All these variables along with the software can impact the accuracy of the reading. As there has been a trend in increased use of CBCT, there has also been a shift towards more digital planning and fabrication of surgical guides according to the depth or "perceived distance" of implant planned in the software.

1.5 Role of software in dental implant planning

Over the past decade, with the aid of CBCT, dentistry has been shifting towards increased digital planning for implant placement. Due to the exponential growth of dental implants, there has also been a similar growth in implant planning softwares (Vercruyssen et al. 2015). This is chiefly due to the allowance of the CBCT manufactures to release the CBCT image datasets into the DICOM format (Vasconcelos et al. 2015). This has led to better communication between many clinicians and non-clinicians for not just implant planning but cases including endodontic treatment and oral pathologies (MacDonald, 2020). Currently, there are numerous third-party softwares in the market that can not only view the DICOM files but have additional options for implant planning. Over the years, these softwares have gotten more sophisticated as multitude of them have an "Implant library" which allows for virtual placement of most of the implants in the

market in the selected trans-axial view of interest. Furthermore, most of these softwares come with a “nerve marking” tool which can be free-handed or auto generated to map out the IAN (mandibular canal). This is of great significance as newer generation of softwares allow us to plan and simulate prior to implant placement. Further advancement of these softwares have led to tools which can allow the clinician to generate a surgical guide which can be used to execute the surgical phase of the implant placement (Vercruyssen et al. 2015). This workflow could benefit the clinician and the patient tremendously as it could theoretically reduce procedure time and discomfort associated with lengthy procedures (Vercruyssen et al. 2015). Tahmaseb et al. (2014) conducted a systematic review to assess the accuracy of software assisted implant placement. They compared the planned position to the actual implant position. The authors noted that there was a mean deviation of 1.12mm and 1.39mm at the entry point and apex respectively, with a mean angular deviation of 3.89 degrees. They also found that maximum reported deviation was approximately 4.5mm and 7.1mm at the entry point and apex respectively, with approximately 21 degrees of angular deviation. Such values are considerable cause of concern. Some of the reasons for inaccuracy include inadequate CBCT image quality, movement of the guide during surgery, patient movement either in scanning or during surgery, motion artifacts, and metal artifacts (Vercruyssen et al. 2015, Tahmaseb et al. 2014). It is important to note that the systematic review covered guides and plans from many different softwares but accuracy of one to another was not done. It was pointed in a recent systematic review by Fokas et al. (2018) that linear accuracy of CBCT may be dependent on exposure parameters and the softwares used in processing the scanned files. For a fully digital workflow, it may be crucial information to know whether performance of one software is superior to another. Currently, there is very limited scientific evidence for the performance of these softwares (Fokas et al. 2018).

1.6 Research Aims

This study has the following aims:

1. To assess the accuracy of four implant planning softwares:

   coDiagnostix, Dental Wings, Canada, parent organization Straumann), DTX Studio Implant (Nobel BioCare, Switzerland), Simplant Pro (Dentspy Sirona, USA), and Blue Sky Plan (Blue Sky Bio, USA) in identifying the mandibular canal using the built in free-hand tool.
2. To determine if voxel size affects the accuracy of these softwares.
3. To determine if mA affects the accuracy of these softwares.
4. To calculate the sensitivity value of softwares as it relates to accuracy.

Our hypothesis is as follows:

Null Hypothesis: There are no differences between different commercially available implant planning (coDiagnostix, DTX studio, Simplant, and Blue Sky Plan) in identifying the mandibular canal in cone beam CT using the free-hand nerve marking tool in the software.

Research Hypothesis: There are differences between different commercially available implant planning (coDiagnostix, DTX studio, Simplant, and Blue Sky Plan) in identifying the mandibular canal in cone beam CT using the free-hand nerve marking tool in the software.

Chapter 2: Materials and Methodology

Application was made to the UBC Anatomical Sciences department for the use of 2 de-fleshed human mandibles for the project. Access to these mandibles were granted after the application to the UBC Anatomical Sciences was deemed successful. Ethics approval certificates were granted for all parts of this study from UBC Clinic Research Ethics Board (Certificate number: H19-02646).

The human mandibles were anonymous donations to the UBC Anatomical Sciences department and no demographic information regarding the age and sex of the subjects were made known. The two mandibles were distinguished by the presence of dentition. “Mandible 1” was given the designation for the dentate mandible and “Mandible 2” for the edentulous mandible and labelled accordingly.

2.1 CBCT scanning protocol and parameters

After obtaining mandibles, steps were taken to ensure proper and consistent seating for obtaining CBCT scans. The machine used for the CBCT scan was the Carestream 9300. The mandibles were fixated to foam insert which was subsequently inserted on a glass slab. The glass slab is directly parallel to the ground horizontal plane. The glass slab was fixated on the bite hold onto the Carestream CBCT machine.

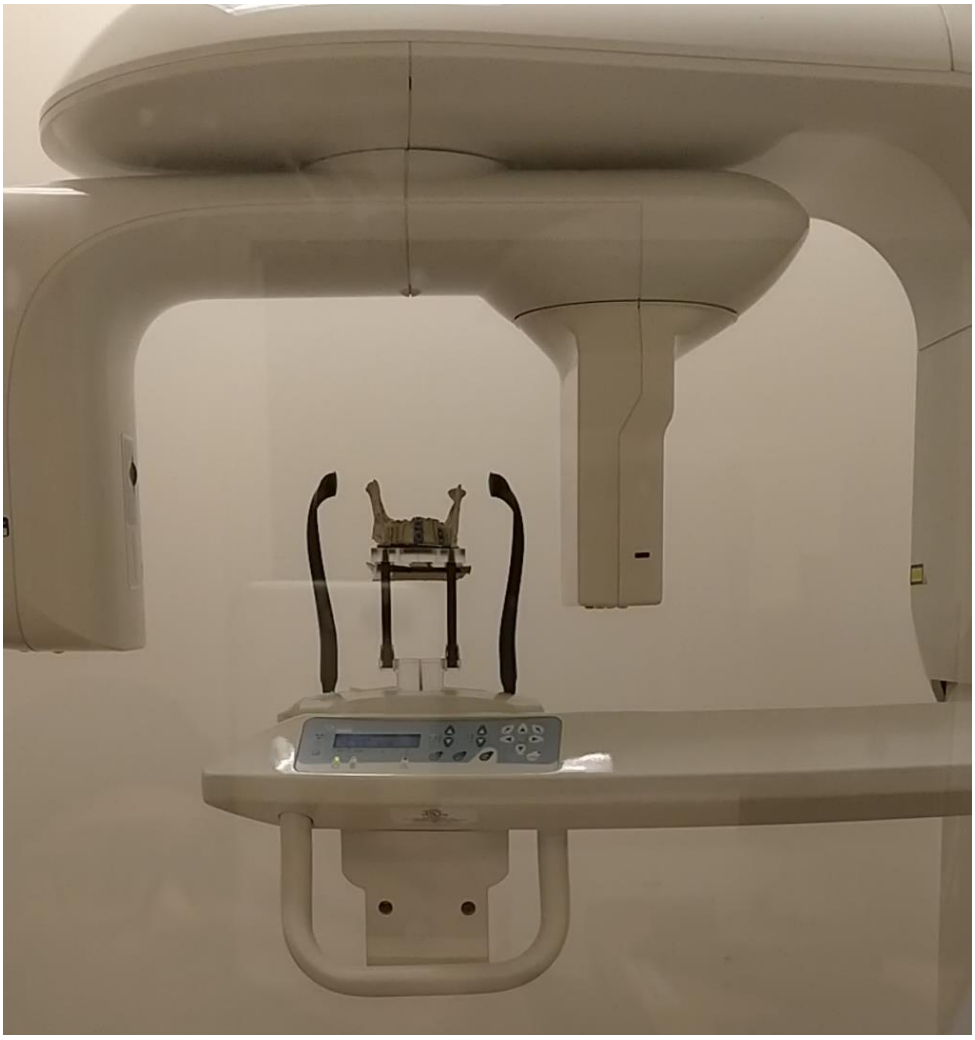

Figure 1 Mandible 1 placed on Carestream 9300

After ensuring standardized placement of the Mandible 1 and Mandible 2 to the inserts, permanent markers were used to mark the superimposed line to depict the horizonal plane and vertical plane over the ramus of the mandible depicting from the CBCT machine. This ensured scans were captured at the same vertical and horizontal plane. Furthermore, this also confirmed that the gnatry angle was unchanged for all of the scans to be taken. In addition, the CBCT machine was rotated and the same vertical plane was used to mark the landmarks of interest in both Mandible 1 and Mandible 2.

The landmarks chosen for the study were similar to prior studies conducting linear measurements for CBCT images (Neves et al. 2014, Dantas el al. 2005).

Landmarks for Mandible 1 included:

RM2 (right second molar)

RM1 (right first molar)

RP2 (right second premolar) : designated in the same plane as mental foramen

RC (right canine)

I (incisor)

LP2 (left second premolar) : designated in the same plane as mental foramen

LM1 (left first molar)

LM2 (left second molar)

Landmarks for Mandible 2 included the regions of the estimated corresponding teeth: Since Mandible 2 is an edentate jaw, an extra site in the proximity of first and second premolar (RP1/RP2) was included to give an additional landmark for the data set. In addition, the site was chosen for it allocation posterior to the mental foramen so linear accuracy to the mandibular canal could be evaluated.

RM2 (right second molar)

RM1 (right first molar)

RP2 (right second premolar)

RP1 (right first premolar) : designated in the same plane as mental foramen

RC (right canine)

LC (left canine)

LP1 (left first premolar) : designated in the same plane as mental foramen

LP2 (left second premolar)

LM1 (left first molar)

LM2 (left second molar)

The vertical planes corresponding to the standardized horizontal plane was superimposed over the selected landmarks and vertical lines marked with black marker. These lines were then either marked using Gutta percha markers or gutta percha points along the buccal aspect of landmarks. In addition, lines were also marked on the lingual aspect and gutta percha marker placed on the superior aspect of the lingual cortex corresponding to the landmark. These are shown in figures 2, 3, 4 and 5

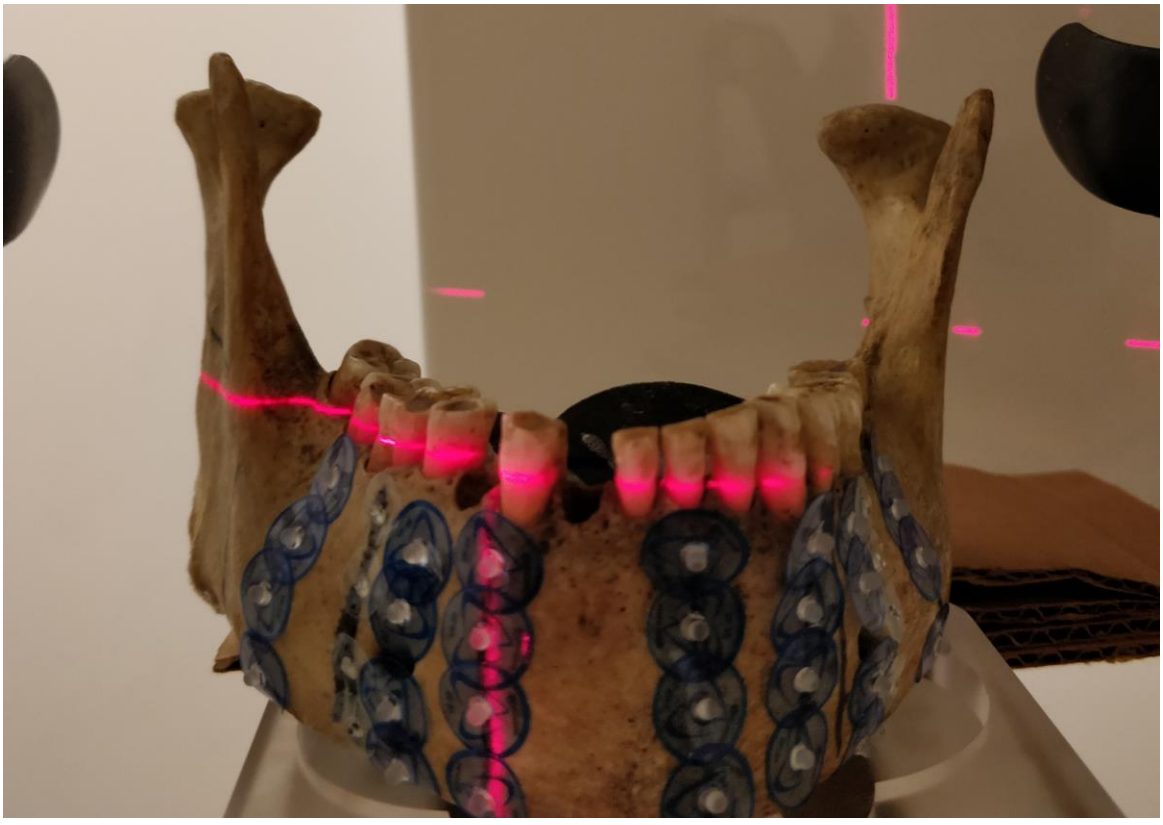

Figure 2 Vertical plane depicting over the marked lines and gutta percha markers on the buccal aspect in Mandible 1

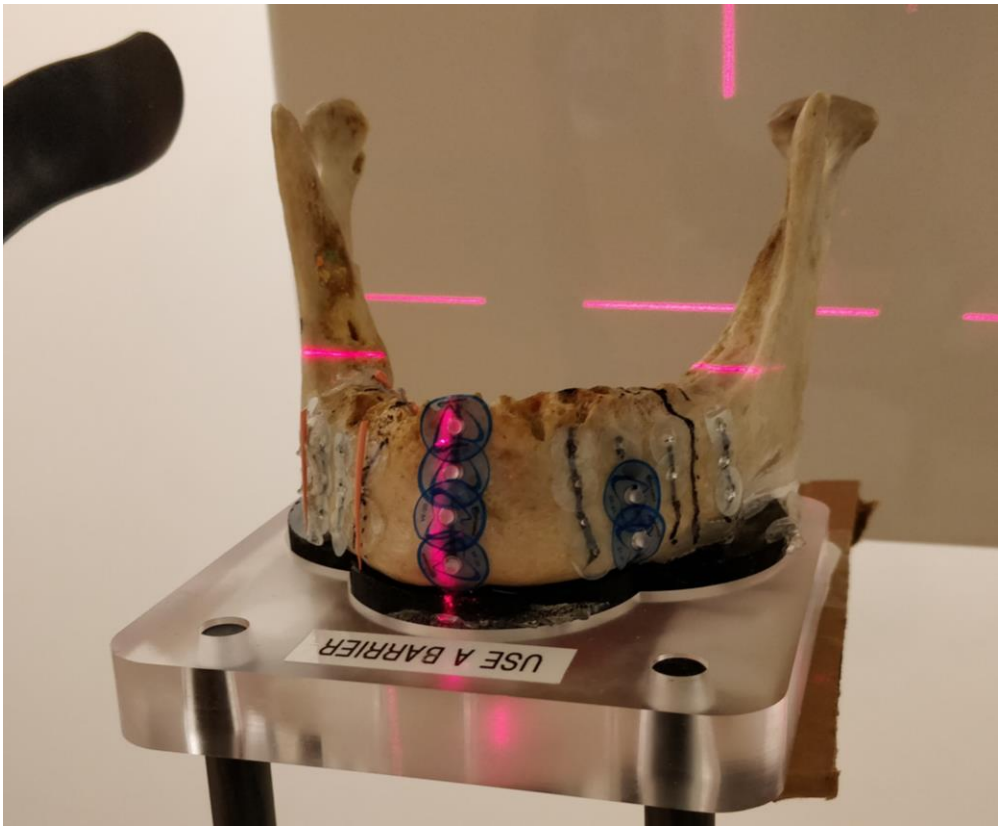

Figure 3 Vertical plane depicting over the marked lines and gutta percha markers on the buccal aspect in Mandible 2

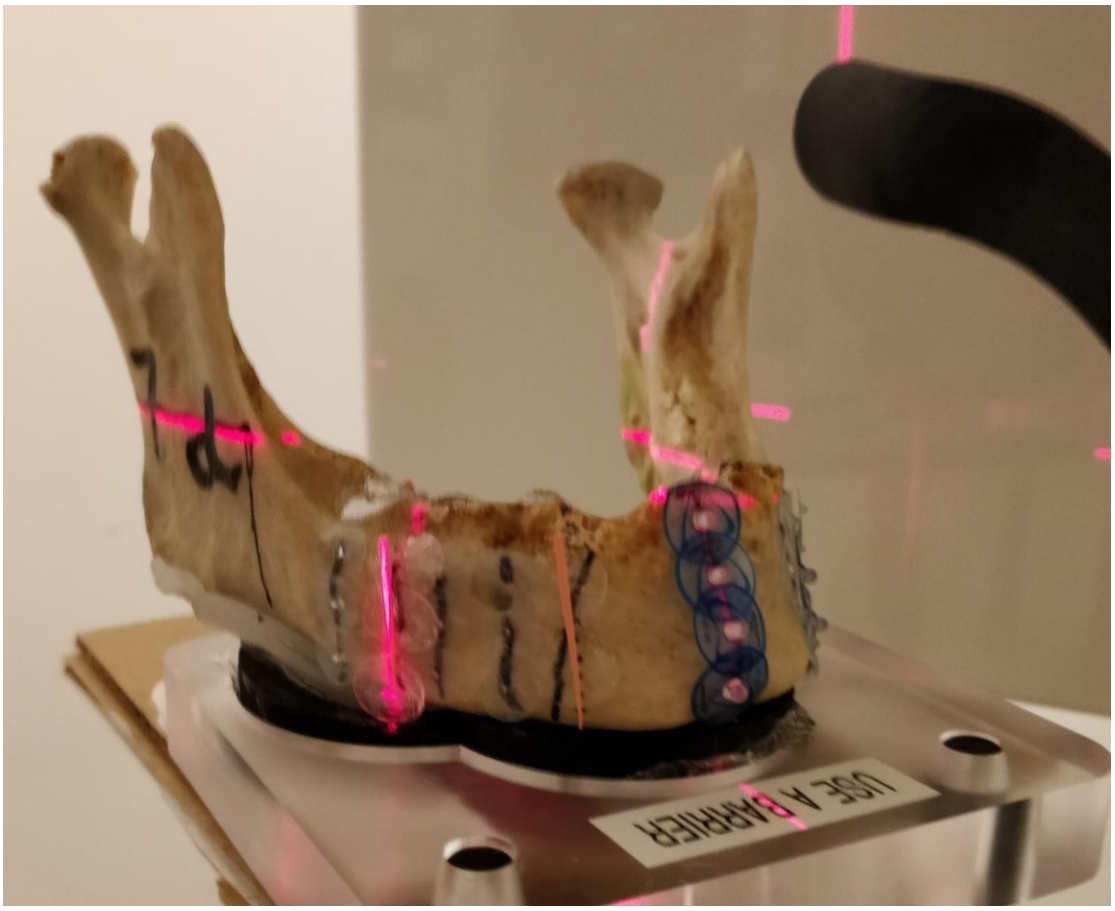

Figure 4 Vertical plane depicting over the marked lines and gutta percha markers on the buccal aspect in Mandible 2

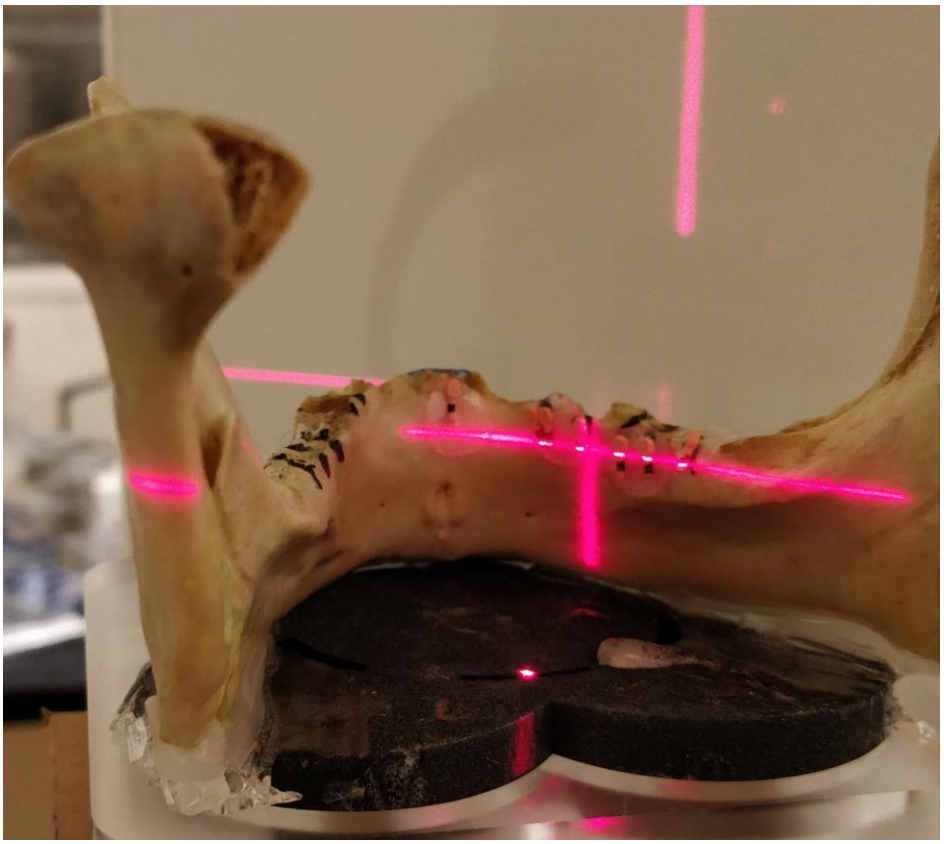

Figure 5 Vertical plane depicting over the marked lines and gutta percha markers on the lingual aspect in Mandible 2

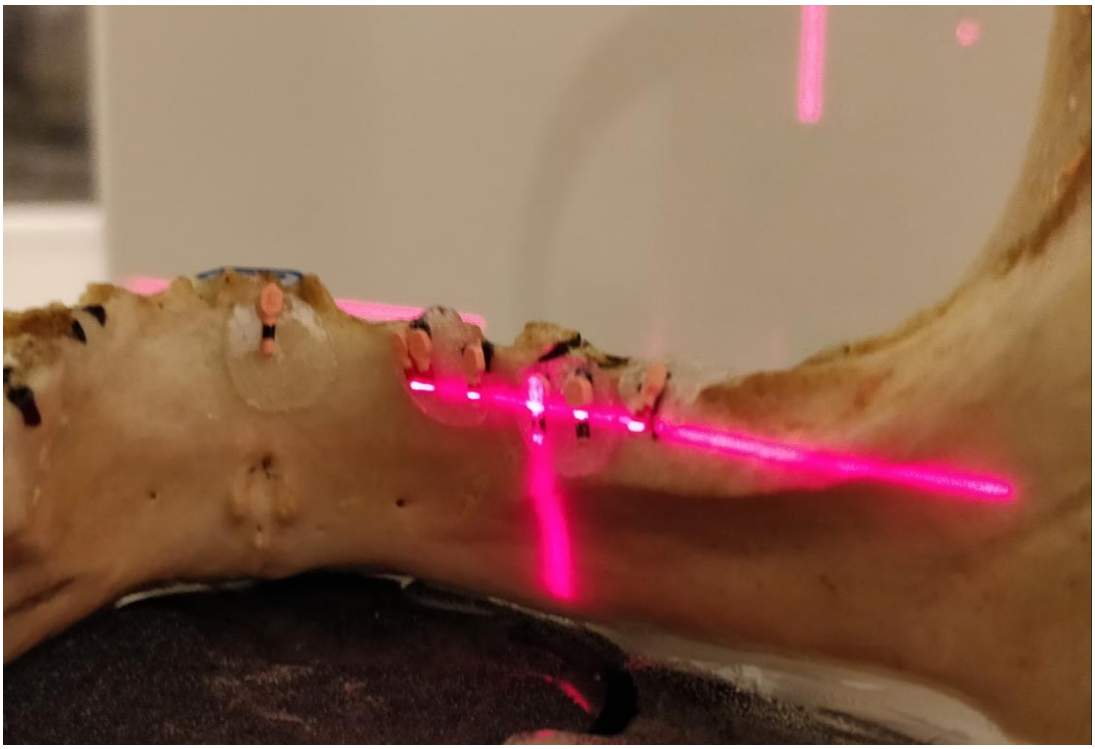

Figure 6 Vertical plane depicting over the marked lines and gutta percha markers on the lingual aspect in Mandible 2

After placement of the gutta percha points and markers, Mandible 1 and 2 were scanned using Kodak Carestream 9300 using the following parameters.

In accordance with the objectives of the study, mA values and voxel values were varied to determine whether change in these parameters would affect the accuracy of the CBCT scans in corresponding softwares.

Each mandible was scanned at the following mA, kVp and voxel sizes. The kVp were values were set at 90. The mA and voxel sizes were manipulated as shown below. Furthermore, all of the scans were taken in 10x10 FOV.

mA	kvP	Voxel
3.2	90	180
4	90	180
5	90	180
3.2	90	300
4	90	300
5	90	300

After each scan, CBCT images were saved as a DICOM files for each of the above parameters.

2.2 CBCT image review and nerve tracing

Each DICOM file was reviewed in the following four softwares:

Software (Manufacturer)
coDiagnostix (Dental Wings, Canada, parent organization Straumann)
DTX Studio Implant (Nobel BioCare, Switzerland)
Simplant Pro (Dentspy Sirona, USA)
Blue Sky Plan (Blue Sky Bio, USA)

Each file was viewed on the same laptop. coDiagnostix, DTX Studio Implant and Blue Sky Plan were installed on the same laptop. Access to Simplant was done via remote access using TeamViewer using the same laptop. Laptop specifications are as follows:

Operating system: Windows 10

Processor: Intel® Core™ i5-7300 CPU @ 2.60GHz 2.71 GHz

Installed RAM: 8.00 GB

System type: 64-bit operating system, x64-based processor.

Mandibular canal was traced using each of the softwares. This was done using curved planar reformation. This was achieved by aligning the long axis of the imaging plane along the mandibular arch. In addition, each of the softwares allow for serial trans-planar reformation which produces a sequence of successive images orthogonal to the curved planar reformation (John et al. 2015). The resultant images are meant to produce images with minimal distortion and subsequently measurements made from the images are presumed to have the least amount of

error (John et al. 2015). No change to the image enhancing feature was used except for contrast and brightness. Nerve was traced using the free-hand tool while simultaneous viewing images in reformatted panoramic image, sagittal, cross-sectional and axial views. An example of the nerve tracing in each software is shown below in figures 7, 8, 9 and 10.

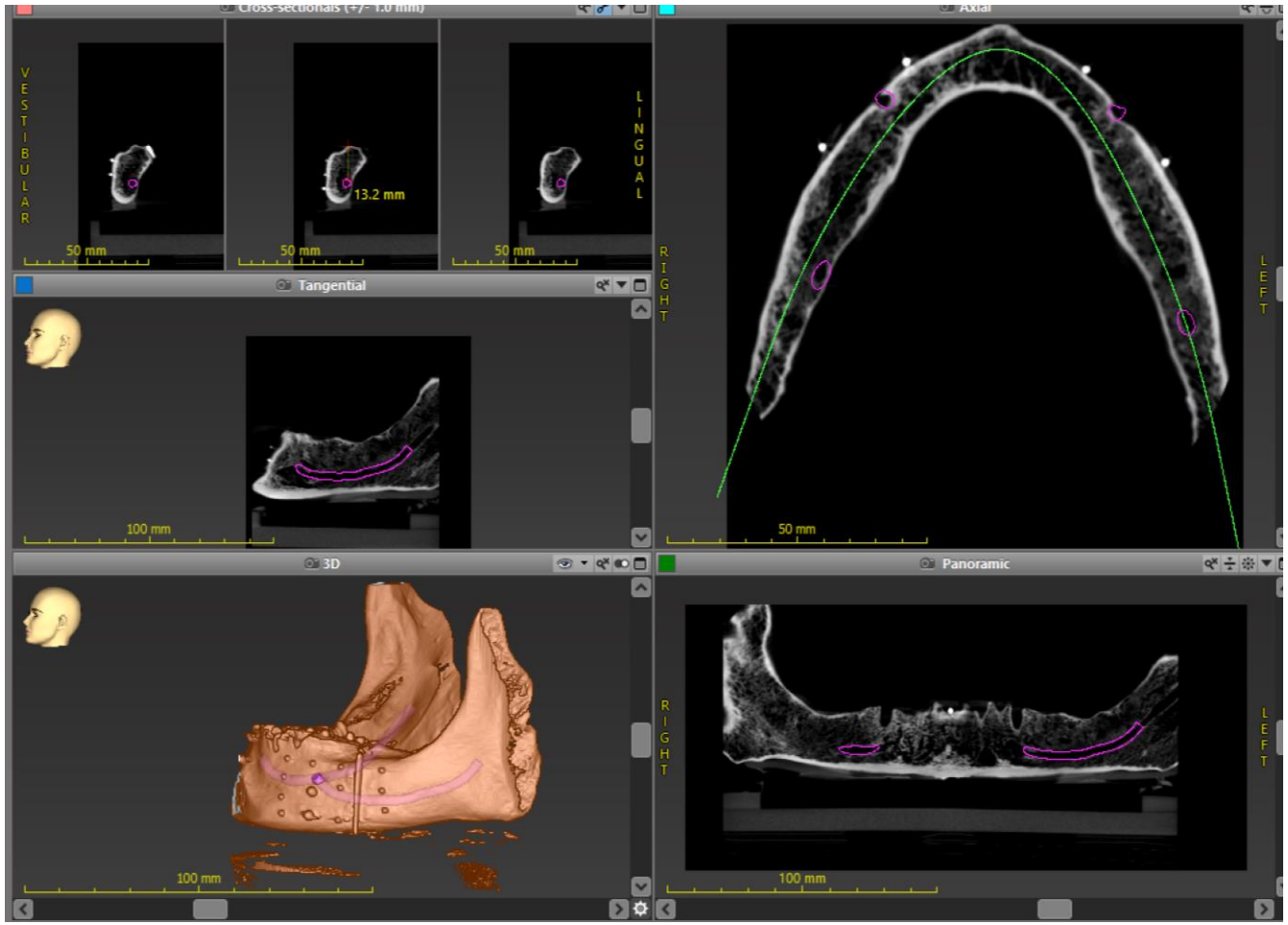

Figure 7 Example of trans-axial, sagittal and Axial views in coDiagnostix software for Mandible 2. Nerve tracing is demonstrated by the purple line.

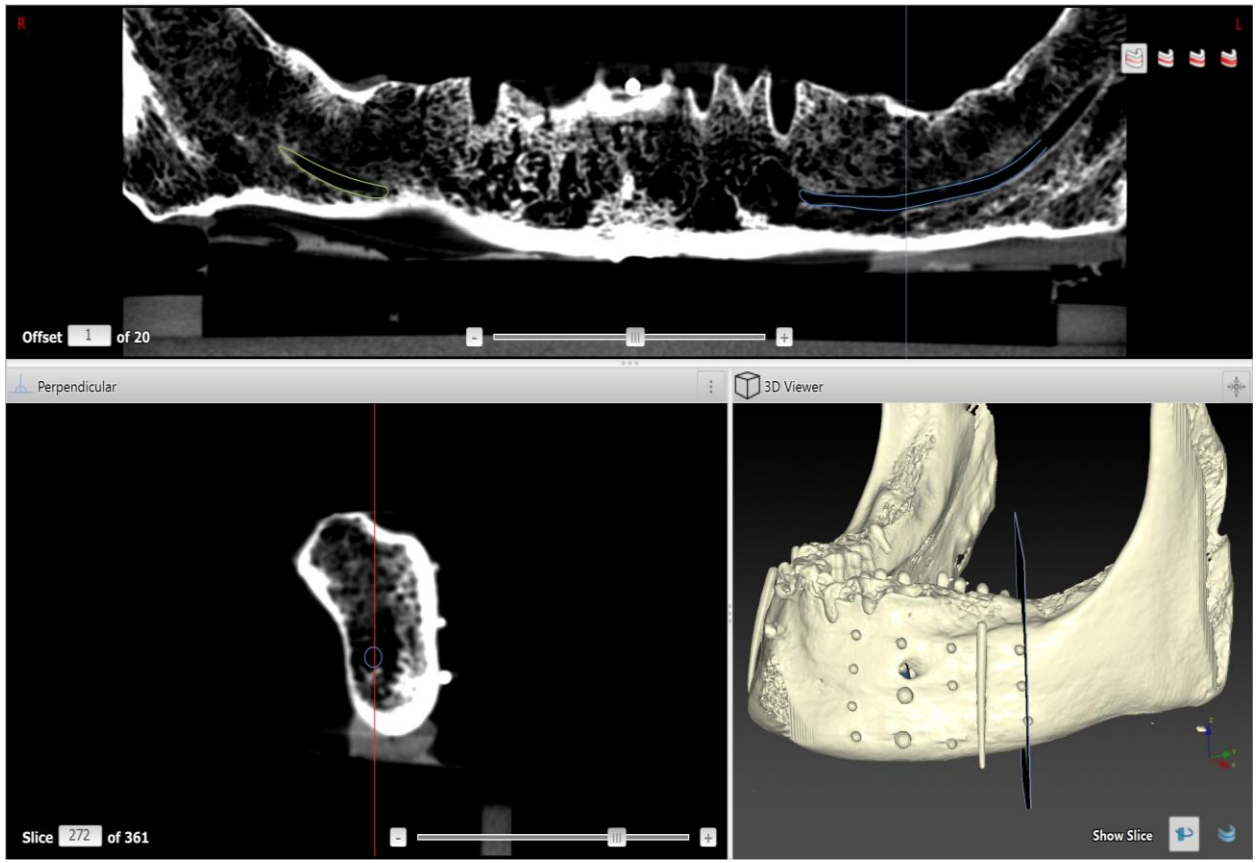

Figure 8 Example of Panoramic and transaxial views along with 3-D rendition in DTX Studio Implant software for Mandible 2. Nerve tracing is demonstrated by the green line in the right hemi-mandible and blue line in left hemi-mandible.

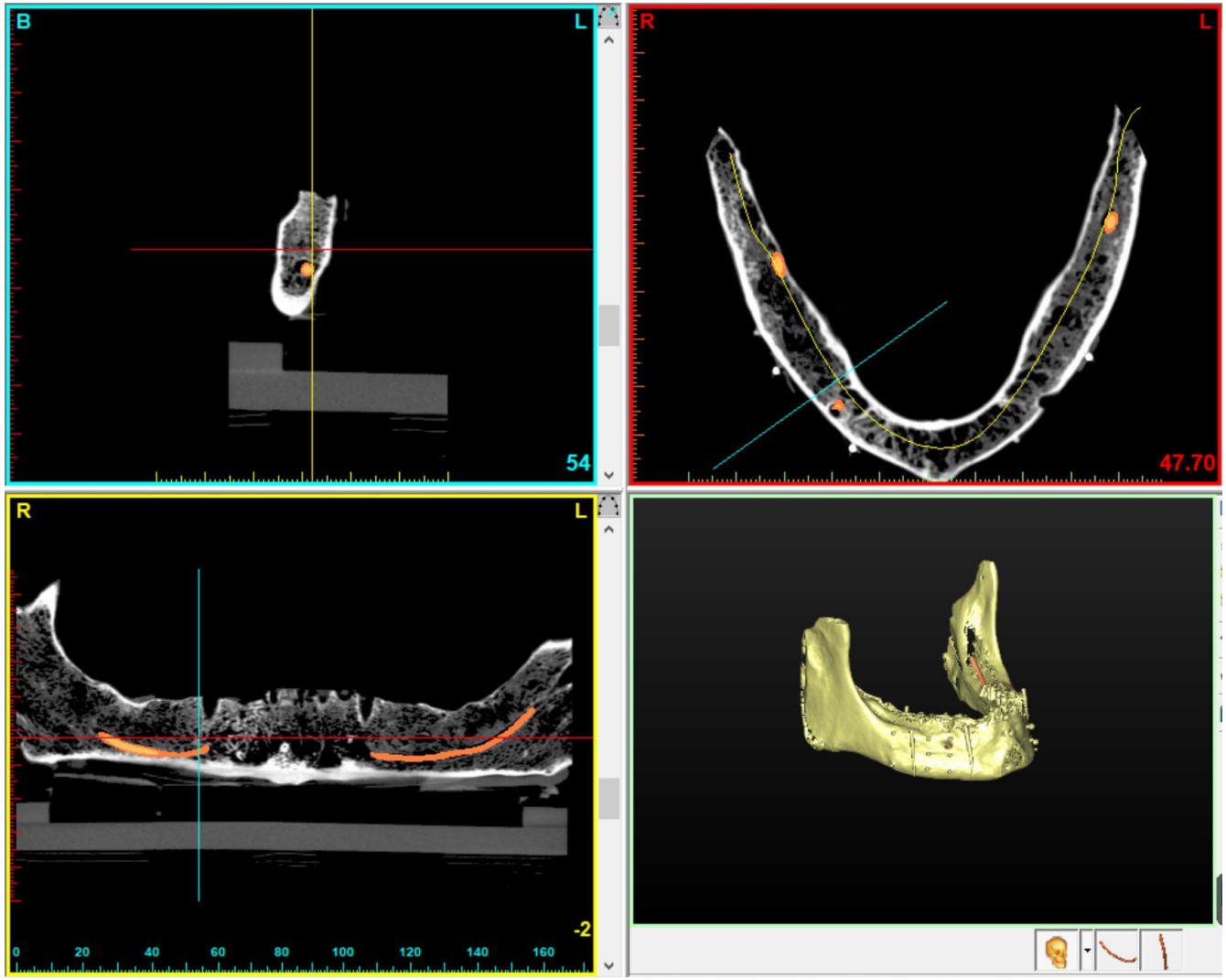

Figure 9 Example of transaxial, sagittal and Axial views in Simplant software for Mandible 2. Nerve tracing is demonstrated by the orange line.

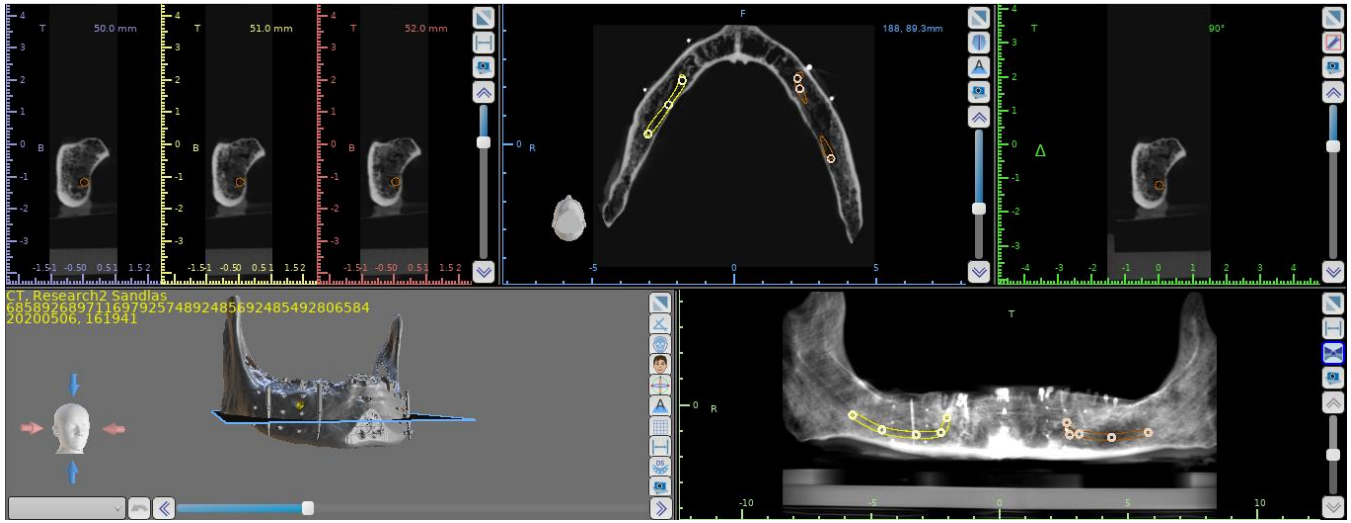

Figure 10 Example of transaxial, sagittal and Axial views in Blue Sky Plan software for Mandible 2. Nerve tracing is demonstrated by the yellow and orange lines.

2.3 CBCT data measurement

Measurements were made using digital measurement tools in the software. At each landmark, sagittal view was aligned using the gutta percha markers. A straight line was made to connect the buccal and lingual segments along the landmarks RM2, RM1, RP2, LP2, LM1, LM2 on mandible 1. The measurement was made from the midpoint connecting the superior aspect of the buccal and lingual cortex whereby measurement line was drawn to the superior aspect of the mandibular nerve. The mandibular nerve was determined by free-hand using the nerve marking tool. This was done in each of the four softwares. An example of the measurements in the softwares is demonstrated in figures 11, 12, 13 and 14 along the same section in Mandible 1.

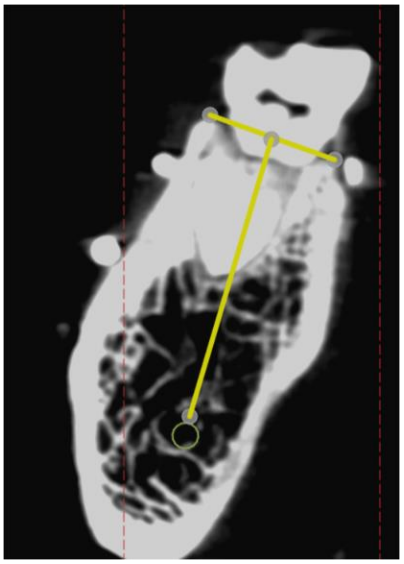

Figure 11 Vol. 20 in DTX at the section of RM2 in Mandible 1 (green circle represents nerve in sagittal section)

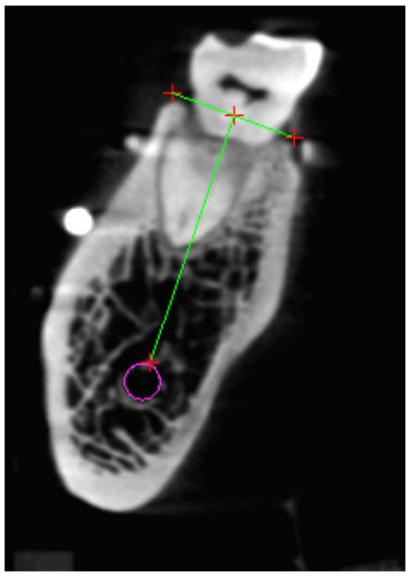

Figure 12 Vol. 20 in coDiagnostix at the section of RM2 in Mandible 1 (purple circle represents nerve in sagittal section)

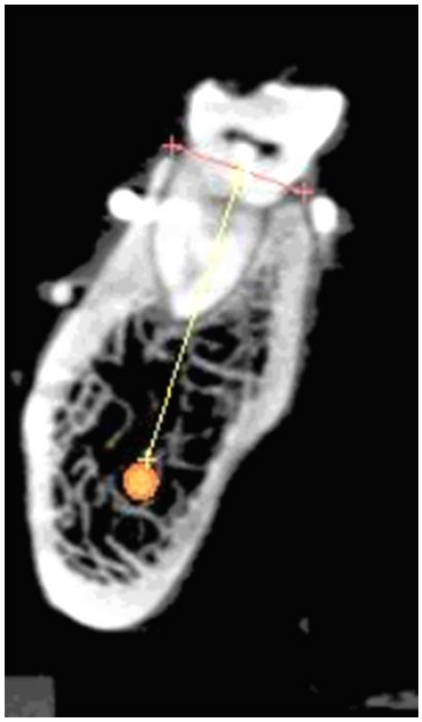

Figure 13 Vol. 20 in Simplant at the section of RM2 in Mandible 1 (orange circle represents nerve in sagittal section)

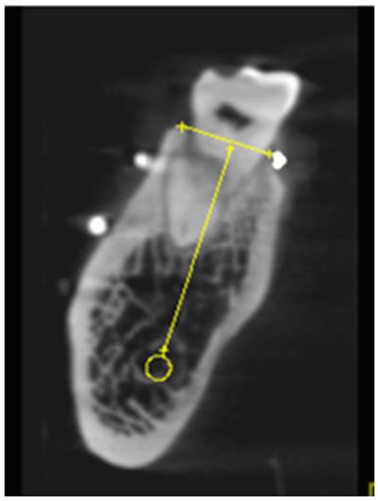

Figure 14 Vol. 20 in Simplant at the section of RM2 in Mandible 1 (orange circle represents nerve in sagittal section)

The line connecting buccal and lingual segments was also made on landmarks RC, I, and LC. The measurement was made from mid-point of the line to the inferior aspect of the cortex along the long axis of the tooth on these landmarks on mandible 1 as the nerve exists the mental foramen along the axis of RP2 on mandible 1.

In Mandible 2, measurements were made from the top of the crest to the superior aspect of the mandibular nerve as determined by free-hand nerve marking tool on landmarks RM2, RM1, RP2, RP1, LP1, LP2, LM1, LM2. An example of the linear measurements is demonstrated in figures 15, 16, 17, and 18.

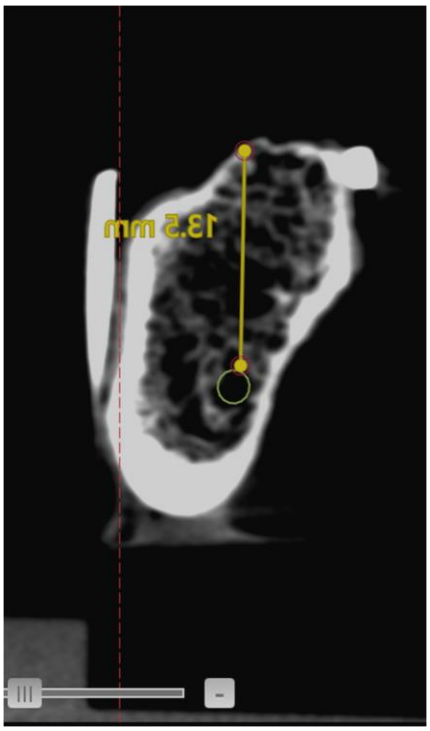

Figure 15 Vol. 8 in DTX studio at the section of RM1 in Mandible 2 (green circle represents nerve in sagittal section)

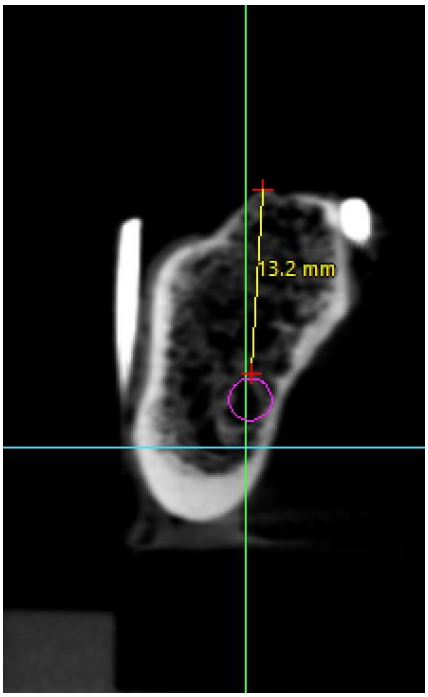

Figure 16 Vol. 8 in coDiagnostix studio at the section of RM1 in Mandible 2 (purpe circle represents nerve in sagittal section)

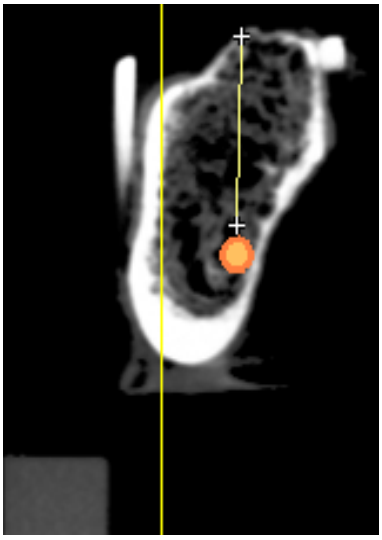

Figure 17 Vol. 8 in Simplant studio at the section of RM1 in Mandible 2 (orange circle represents nerve in sagittal section)

Figure 18 Vol. 8 in Blue Sky Plan at the section of RM1 in Mandible 2 (orange circle represents nerve in sagittal section)

In addition, the measurements were made from the most superior aspect of the crest to the most inferior aspect of the crest along the landmarks RC and LC. An example of the linear measurements in this section is demonstrated in Fig. 19, 20, 21, and 22.

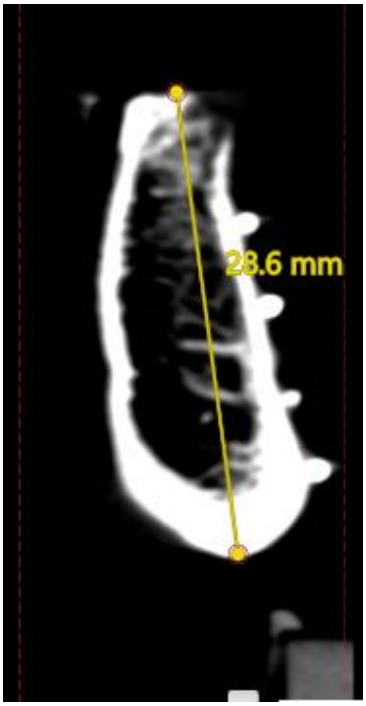

Figure 19 Vol. 8 in DTX (measurement being made from the most superior aspect to the most inferior aspect)

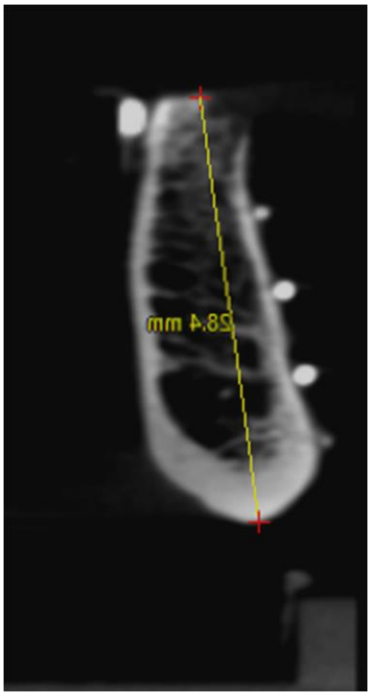

Figure 20 Vol. 8 in coDiagnostix (measurement being made from the most superior aspect to the most inferior aspect)

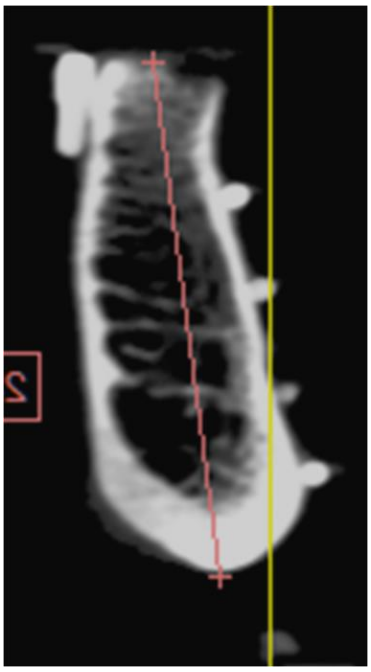

Figure 21 Vol. 8 in Simplant (measurement being made from the most superior aspect to the most inferior aspect)

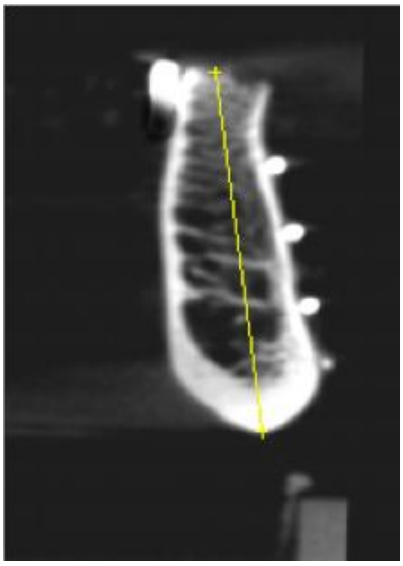

Figure 22 Vol. 8 in Blue Sky plan (measurement being made from the most superior aspect to the most inferior aspect)

2.4 Mandible sectioning

The mandibles were stabilized to the cutting board using two Irwin Quick-grips. The mandibles were sectioned along the desired planes using Walter Super 5 PS grinder and the

Walter Zipone 11-T 552 disc measuring 125mm x 22/23mm x 1mm (in thickness). At each section of the mandible, digital calipers with an accuracy of 0.01mm were used to the record the measurement along the corresponding landmarks to achieve the gold standard.

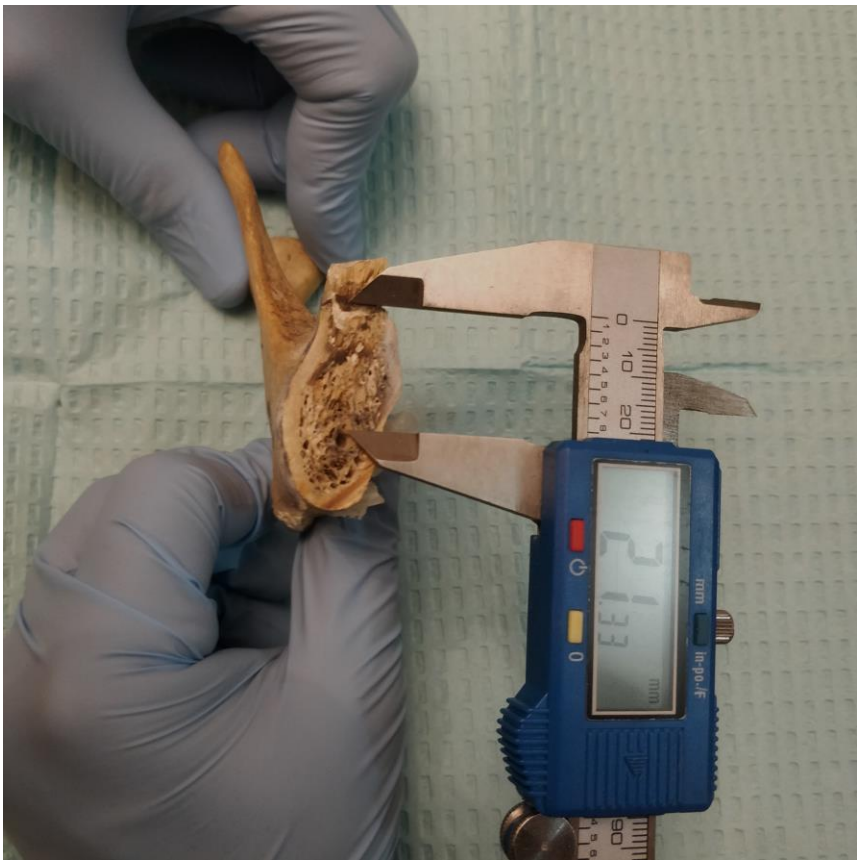

Figure 23 Measurement from the midpoint of the buccal and lingual cortex along the cross-section at RM2 in Mandible 1 using the digital caliper

2.5 Statistical Analysis

Three-way ANOVA was used to compare the means of the three grouping variables (mA, kVp and softwares) on the accuracy (independent variable). Two-way ANOVA was also used to compare the means of each CBCT parameter and corresponding software to the caliper readings. Paired t-tests was used to compare the differences between Mandible 1 and Mandible 2.

Sensitivity values were calculated using threshold values. Furthermore, Tukey's HSD was used as a post-hoc test to determine whether there was a significant difference in accuracy when comparing one software to another.

Chapter 3: Results

3.1 Data Evaluation

All of the images pertaining the corresponding sections mentioned in Chapter 2 were measured in all of the four softwares. Each section in each software was measured twice. Each reading was taken atleast 3-4 weeks apart to avoid bias.

ICC was calculated and was noted to be 0.989 for the readings. Calculation for the intra-examiner reliability is provided in appendix B.

The data and the tables in Section 3.2 provide an average of the two different readings. Subsequently the average at each location was compared to the caliper "gold standard". The "difference" in the tables (Section 3.2) provided is the measurement readings in the softwares subtracted from caliper readings. Therefore, the difference of zero represents that the distance measured in the software is the same as the caliper measurement. A negative value represents an overestimation of the measurement by the software. A positive value represents an underestimation of the measurement by the software.

3.2 Caliper vs. CBCT Parameters

The highlighted numbers of the mean differences in tables of this section showed statistical difference values from Two-way ANOVA analysis comparing the mean difference between the software readings and the caliper measurements at different locations. Two-way ANOVA data tables are attached in Appendix D. Statistical difference is calculated below threshold value of the 95% confidence interval of difference which also accounts for the variance of the two reading measurements. P value set at (<0.05). This is important to note and observe. An example for this is given as follows: Let's assume that if a caliper gold standard reading is 3mm for given a location. Measurements in Software 1 are 2mm for first reading and 4mm for

second reading. The mean would be calculated to 3mm for Software 1. Measurement for Software 2 are 1mm for first reading and 5mm for second readings. The mean would also be calculated to 3mm. Just by observing the mean, one would assume that Software 1 and 2 are equal however variance in Software 2 is considerably higher and may result in higher probability of inaccurate readings than Software 1. This is also accounted for the statistical difference observed in Tables below where some values tend to have similar mean differences but do not display statistical difference when taking variance of the readings into account.

The raw data tables for Mandible 1 and Mandible 2 are attached in the appendix A (subsection .1 and .2) including the first and the second readings. In addition, the gold standard tables are attached in the appendix A (subsection .3) as well. Two-way ANOVA analysis of the data is attached in Appendix D.

3.2.1 Caliper vs. 3.2 mA 180 Voxel

Table 1: Caliper vs 3.2 mA 180 Voxel in Mandible 1 (Distance measured in mm)

Location	Caliper	3.2mA 180Voxel DTX	SD±	Difference	3.2mA 180Voxel coD	SD±	Difference	3.2mA 180Voxel BSP	SD±	Difference	3.2mA 180Voxel SM	SD±	Difference
RM2	21.23	22.5	0	-1.27	22.15	±0.07	-0.92	22.1	±0.08	-0.87	22.05	±0.16	-0.82
RM1	22.54	22.8	±0.57	-0.26	22.5	±0.71	0.04	22.13	±0.76	0.41	21.7	±0.4	0.84
RP2	16.5	15.85	±1.48	0.65	16.55	±0.21	-0.05	16.43	±0.3	0.07	16.02	±0.21	0.48
RC	36.68	36.8	±0.57	-0.12	36.75	±0.35	-0.07	35.17	±0.46	1.51	35.69	±0.65	0.99
I	35.19	35.45	±0.35	-0.26	36.35	±0.21	-1.16	34.78	±0.45	0.41	35.67	±0.22	-0.48
LC	35.1	36.2	±0.85	-1.1	36.3	±0	-1.2	36.67	±0.86	-1.57	35.98	±0.09	-0.88
LP2	17.28	16.85	±1.34	0.43	16.75	±0.35	0.53	16.23	±0.06	1.05	16.89	±0.23	0.39
LM1	23.29	23.75	±0.35	-0.46	23.15	±0.78	0.14	23.43	±0.16	-0.14	22.62	±0.93	0.67
LM2	22.78	22.4	±0.14	0.38	22.4	±0.28	0.38	22.8	±0.66	-0.02	22.16	±0.49	0.62

Table 2: Caliper vs 3.2 mA 180 Voxel in Mandible 2 (Distance measured in mm)

Location	Caliper	3.2mA 180Voxel DTX	SD±	Difference	3.2mA 180Voxel coD	SD±	Difference	3.2mA 180Voxel BSP	SD±	Difference	3.2mA 180Voxel SM	SD±	Difference
RM2	13.73	13.65	±0.78	0.08	13.2	±0.42	0.53	13.435	±0.26	0.295	12.95	±0.23	0.78
RM1	13.22	13.35	±0.21	-0.13	13.25	±0.07	-0.03	13.255	±0.18	-0.035	13.565	±0.09	-0.345
RP2	13.72	14	±0.14	-0.28	13.8	±0.14	-0.08	13.58	±0.4	0.14	13.57	±0.37	0.15
RP1	12.58	12.6	±0.14	-0.02	13.5	±0.14	-0.92	13.645	±0.04	-1.065	12.405	±0.04	0.175
RC	26.51	25.25	±0.49	1.26	25.8	±0.14	0.71	25.545	±0.42	0.965	26.055	±0.22	0.455
LC	28.12	28.25	±0.49	-0.13	28.5	±0.14	-0.38	27.825	±0.12	0.295	28.225	±0.06	-0.105
LP1	10.32	9.8	±0.42	0.52	10.05	±0.07	0.27	9.915	±0.63	0.405	10.185	±0.15	0.135
LP2	13.91	14.5	±0.28	-0.59	13.9	±0.57	0.01	14.83	±0.31	-0.92	14.075	±0.35	-0.165
LM1	14.36	14.05	±0.35	0.31	13.65	±0.35	0.71	14.065	±0.35	0.295	13.31	±0.27	1.05
LM2	13.12	13.35	±0.64	-0.23	13.35	±0.21	-0.23	13.205	±0.86	-0.085	11.755	±0.64	1.365

The results of the caliper and the different anatomical locations are listed in the Table 1 and 2 for Mandible 1 and Mandible 2 respective where the CBCT parameters are set at 3.2mA with 180 Voxel. The numbers highlight in yellow demonstrate the statistically significant mean differences between noted between software measurements and caliper. Significant differences are noted at RM2 for DTX. coD shows a statistically significant difference at LC at a difference of -1.2mm from the caliper reading. BSP shows a statistically significant difference at LP2 with a mean difference of 1.05mm. No statistical difference is noted for the SM. For Mandible 2, the only statistical difference is noted at RP1 for BSP at difference -1.065mm.

In Mandible 1, only 5 out the of the 36 mean values had a difference greater than 1mm. In Mandible 2, only 4 out of the 40 mean values had a difference greater than 1mm. These values are highlighted in purple.

3.2.2 Caliper vs. 4mA 180 Voxel

Table 3: Caliper vs. 4.0mA and 180 Voxel at Different locations in Mandible 1 (Distance measured in mm)

Location	Caliper	4mA 180Voxel DTX	SD±	Difference	4mA 180Voxel coD	SD±	Difference	4mA 180Voxel BSP	SD±	Difference	4mA 180Voxel SM	SD±	Difference
RM2	21.23	22.45	±0.07	-1.22	22.5	±0.35	-1.27	22.04	±0.3	-0.81	21.655	±0.51	-0.425
RM1	22.54	22.75	±0	-0.21	22.05	±1.13	0.49	23.02	±0.39	-0.48	22.215	±0.31	0.325
RP2	16.5	16.1	±1.84	0.4	16.05	±0.21	0.45	15.815	±0.22	0.685	15.355	±0.61	1.145
RC	36.68	37.15	±0.28	-0.47	35.5	±0.57	1.18	35.44	±0.81	1.24	36.12	±0.28	0.56
I	35.19	35.3	±0.07	-0.11	35.65	±0.14	-0.46	34.66	±0.76	0.53	35.74	±0.49	-0.55
LC	35.1	36.65	±0	-1.55	36.2	±0.92	-1.1	36.32	±1.11	-1.22	36.88	±0.65	-1.78
LP2	17.28	16.6	±0.35	0.68	17.15	±0.14	0.13	16.355	±0.08	0.925	17.3	±0.16	-0.02
LM1	23.29	23.6	±0.92	-0.31	23	±0.07	0.29	23.195	±0.47	0.095	23.4	±0.47	-0.11
LM2	22.78	22.6	±0.78	0.18	22.55	±0.71	0.23	21.985	±0.21	0.795	22.74	±0.16	0.04

Table 4: Caliper vs. 4.0mA and 180 Voxel at Different locations in Mandible 2 (Distance measured in mm)

Location	Caliper	4mA 180Voxel DTX	SD±	Difference	4mA 180Voxel coD	SD±	Difference	4mA 180Voxel BSP	SD±	Difference	4mA 180Voxel SM	SD±	Difference
RM2	13.73	13.25	±0.49	0.48	13.25	±0.07	0.48	12.605	±0.57	1.125	12.825	±0.56	0.905
RM1	13.22	13.45	±0.64	-0.23	13.75	±0.21	-0.53	13.06	±0.34	0.16	13.09	±0.96	0.13
RP2	13.72	13.65	±0.07	0.07	13.55	±0.78	0.17	13.475	±0.49	0.245	13.515	±0.06	0.205
RP1	12.58	12.2	±0	0.38	13.4	±0.42	-0.82	13.055	±0.25	-0.475	13.075	±0.54	-0.495
RC	26.51	25.6	±0.57	0.91	25.65	±0.64	0.86	25.15	±0.23	1.36	25.89	±0.01	0.62
LC	28.12	28.35	±0.21	-0.23	28.15	±0.21	-0.03	27.09	±0.06	1.03	27.715	±0.3	0.405
LP1	10.32	9.65	±0.21	0.67	10.1	±0.42	0.22	9.135	±0.19	1.185	10.04	±0.16	0.28
LP2	13.91	14.5	±0.14	-0.59	14.45	±0.49	-0.54	14.74	±0.3	-0.83	13.565	±0.37	0.345
LM1	14.36	14	±0.14	0.36	14.05	±0.07	0.31	13.9	±0.59	0.46	13.425	±0.05	0.935
LM2	13.12	13.75	±0.35	-0.63	12.9	±0.42	0.22	13.68	±0.2	-0.56	12.985	±1.08	0.135

The results of the caliper and the different anatomical locations are listed in the Table 3 and 4 for Mandible 1 and Mandible 2 respective where the CBCT parameters are set at 4.0mA with 180 Voxel. The only statistical difference is noted at RP1 for DTX at mean difference of -1.22mm. No other softwares showed a statistical difference between caliper readings and measurements on the softwares in Mandible 1. For Mandible 2, DTX showed a statistical difference at RP1 at 0.38mm. BSP showed a statistical difference at LC of 1.03mm. SM showed a statistical difference at RC and LM1 at difference of 0.62mm and 0.935mm respectively. No statistical difference was noted between caliper readings and software measurements made in coD.

In Mandible 1, only 7 out the of the 36 mean values had a difference greater than 1mm. In Mandible 2, only 4 out of the 40 mean values had a difference greater than 1mm. These values are highlighted in purple.

3.2.3 Caliper vs 5mA 180 Voxel

Table 5: Caliper vs. 5.0mA and 180 Voxel at Different locations in Mandible 1 (Distance measured in mm)

Location	Caliper	5mA 180Voxel DTX	SD±	Difference	5mA 180Voxel coD	SD±	Difference	5mA 180Voxel BSP	SD±	Difference	5mA 180Voxel SM	SD±	Difference
RM2	21.23	23.15	±0.78	-1.92	22.25	±0.78	-1.02	22.315	±0.73	-1.085	21.365	±0.39	-0.135
RM1	22.54	22.95	±0.35	-0.41	21.9	±0.71	0.64	22.39	±0.91	0.15	22.21	±0.37	0.33
RP2	16.5	15.95	±1.06	0.55	16.4	±0.14	0.1	15.875	±0.05	0.625	15.9	±0.74	0.6
RC	36.68	37.05	±0.07	-0.37	35.75	±0.49	0.93	35.665	±1.66	1.015	36.315	±0.84	0.365
I	35.19	35.1	±0.28	0.09	35.9	±0.42	-0.71	34.385	±0.49	0.805	35.775	±0.88	-0.585
LC	35.1	36.8	±0.28	-1.7	36.65	±0.64	-1.55	35.965	±0.52	-0.865	36.95	±0.17	-1.85
LP2	17.28	17.15	±0.92	0.13	17.35	±0.07	-0.07	16.55	±0.44	0.73	16.84	±0.74	0.44
LM1	23.29	23.85	±0.64	-0.56	23.4	±0.85	-0.11	23.23	±0.17	0.06	23.585	±0.66	-0.295
LM2	22.78	22.7	±0.28	0.08	22.95	±0.07	-0.17	22.595	±0.33	0.185	22.135	±0.15	0.645

Table 6: Caliper vs. 5.0mA and 180 Voxel at Different locations in Mandible 2 (Distance measured in mm)

Location	Caliper	5mA 180Voxel DTX	SD±	Difference	5mA 180Voxel coD	SD±	Difference	5mA 180Voxel BSP	SD±	Difference	5mA 180Voxel SM	SD±	Difference
RM2	13.73	13.8	±0.28	-0.07	13.45	±0.64	0.28	13.42	±0.14	0.31	13.065	±0.05	0.665
RM1	13.22	13.55	±1.06	-0.33	13.15	±0.21	0.07	13.255	±0.45	-0.035	13.435	±0.05	-0.215
RP2	13.72	13.35	±0.21	0.37	13.95	±0.21	-0.23	13.72	±0.01	0	13.675	±0.04	0.045
RP1	12.58	12.2	±0.14	0.38	12.65	±0.64	-0.07	12.72	±0.25	-0.14	12.535	±0.63	0.045
RC	26.51	26.05	±0.21	0.46	25.6	±0	0.91	25.32	±0.04	1.19	25.865	±0.16	0.645
LC	28.12	28.05	±0.35	0.07	28.3	±0.14	-0.18	27.285	±0.25	0.835	28.25	±0.52	-0.13
LP1	10.32	9.55	±0.35	0.77	10	±0	0.32	9.845	±0.5	0.475	9.56	±0.23	0.76
LP2	13.91	13.8	±0.42	0.11	14.5	±0.85	-0.59	14.045	±0.19	-0.135	13.655	±0.28	0.255
LM1	14.36	13.25	±0.07	1.11	13.7	±0.14	0.66	13.815	±0.52	0.545	13.055	±0.09	1.305
LM2	13.12	12.9	±0	0.22	13.4	±0.28	-0.28	12.98	±0.24	0.14	13.12	±0.58	0

The results of the caliper and the different anatomical locations are listed in the Table 5 and 6 for Mandible 1 and Mandible 2 respective where the CBCT parameters are set at 5.0mA with 180 Voxel. No statistical significant differences were noted between caliper readings and softwares in Mandible 1. In Mandible 2, statistical difference was noted at RC for coD and BSP at 0.91mm and 1.19mm, respectively. In addition, at LM1 there was a statistical difference of 1.1mm for DTX. No statistical differences were noted between caliper readings and SM.

In Mandible 1, only 6 out the of the 36 mean values had a difference greater than 1mm. In Mandible 2, only 3 out of the 40 mean values had a difference greater than 1mm. These values are highlighted in purple

3.2.4 Caliper vs 3.2mA 300 Voxel

Table 7: Caliper vs. 3.2mA and 300 Voxel at Different locations in Mandible 1 (Distance measured in mm)

Location	Caliper	3.2mA 300Voxel DTX	SD±	Difference	3.2mA 300Voxel coD	SD±	Difference	3.2mA 300Voxel BSP	SD±	Difference	3.2mA 300Voxel SP	SD±	Difference
RM2	21.23	22.55	±0.07	-1.32	22.55	±0.35	-1.32	21.665	±0.59	-0.435	21.98	±0.78	-0.75
RM1	22.54	22.9	±0.57	-0.36	21.65	±0.49	0.89	22.275	±0.18	0.265	22.195	±0.21	0.345
RP2	16.5	15.85	±0.49	0.65	16.3	±0.85	0.2	15.485	±0.33	1.015	16.67	±0.54	-0.17
RC	36.68	36.1	±0.42	0.58	35.85	±1.34	0.83	35.47	±1.3	1.21	35.44	±0.11	1.24
I	35.19	35.5	±0.57	-0.31	35.8	±0.71	-0.61	35.42	±0.25	-0.23	35.605	±0.09	-0.415
LC	35.1	36.8	±0.42	-1.7	36.75	±0.07	-1.65	35.485	±0.19	-0.385	37.335	±0.45	-2.235
LP2	17.28	16.6	±0.28	0.68	17.5	±0.28	-0.22	16.57	±0.96	0.71	17.405	±0.4	-0.125
LM1	23.29	24.1	±0.28	-0.81	23.75	±0.64	-0.46	23.46	±0.04	-0.17	23.7	±0.75	-0.41
LM2	22.78	22.75	±0.35	0.03	22.3	±0.14	0.48	22.375	±0.62	0.405	22.515	±0.01	0.265

Table 8: Caliper vs. 3.2mA and 300 Voxel at Different locations in Mandible 2 (Distance measured in mm)

Location	Caliper	3.2mA 300Voxel DTX	SD±	Difference	3.2mA 300Voxel coD	SD±	Difference	3.2mA 300Voxel BSP	SD±	Difference	3.2mA 300Voxel SM	SD±	Difference
RM2	13.73	14	±0.28	-0.27	13.35	±0.35	0.38	13.04	±0.01	0.69	13.06	±0.14	0.67
RM1	13.22	13.65	±0.78	-0.43	14	±0.71	-0.78	13.14	±0.17	0.08	13.19	±0.06	0.03
RP2	13.72	14.05	±0.49	-0.33	13.9	±0.14	-0.18	13.775	±0.32	-0.055	13.635	±0.28	0.085
RP1	12.58	12.05	±0.07	0.53	13.2	±0.14	-0.62	13.37	±0.13	-0.79	12.685	±0.84	-0.105
RC	26.51	25.85	±0.35	0.66	25.8	±0.71	0.71	25.895	±0.06	0.615	26.015	±0.29	0.495
LC	28.12	28.7	±0.14	-0.58	28.4	±0.14	-0.28	27.9	±0.01	0.22	28.21	±0.04	-0.09
LP1	10.32	9.75	±0.07	0.57	10.1	±0.28	0.22	9.425	±0.02	0.895	10.14	±0.61	0.18
LP2	13.91	14.45	±0.35	-0.54	14.25	±0.49	-0.34	14.27	±0.1	-0.36	14.115	±0.19	-0.205
LM1	14.36	13.7	±0	0.66	13.6	±0.99	0.76	13.86	±0.21	0.5	13.455	±0.16	0.905
LM2	13.12	12.9	±0	0.22	13.35	±0.49	-0.23	12.88	±0.64	0.24	13.155	±0.36	-0.035

The results of the caliper and the different anatomical locations are listed in the Table 7 and 8 for Mandible 1 and Mandible 2 respective where the CBCT parameters are set at 3.2mA with 300 Voxel. Statistical difference is noted at RM2 for DTX at -1.32mm. At location I, statistical difference is noted for coD at -1.65mm. For SM, statistical difference is observed at LM2 at 0.265mm. No statistical difference is noted for BSP at any locations in Mandible 1. In Mandible 2, statistical difference was noted at RM2 is observed for coD at 0.38mm. At LC and LP1, statistical significant difference is noted in BSP at 0.22mm and 0.895mm respectively. At LM1 and LM2, statistical significant difference is noted for DTX at 0.66mm and 0.22mm respectively. No statistically significant differences were noted in SM in Mandible 2.

In Mandible 1, only 7 out the of the 36 mean values had a difference greater than 1mm. In Mandible 2, no values with a difference greater than 1mm was noted. These values are highlighted in purple

3.2.5 Caliper vs. 4mA 300 Voxel

Table 9: Caliper vs. 4.0mA and 300 Voxel at Different locations in Mandible 1 (Distance measured in mm)

Location	Caliper	4mA 300Voxel DTX	SD±	Difference	4mA 300Voxel coD	SD±	Difference	4mA 300Voxel BSP	SD±	Difference	4mA 300Voxel SP	SD±	Difference
RM2	21.23	22.05	±0.07	-0.82	21.95	±0.35	-0.72	22.285	±0.3	-0.335	22.19	±0.51	-0.24
RM1	22.54	22.6	±0	-0.06	22.2	±1.13	0.34	22.415	±0.39	-0.215	22.38	±0.31	-0.18
RP2	16.5	16	±1.84	0.5	16.45	±0.21	0.05	15.785	±0.22	0.665	16.21	±0.61	0.24
RC	36.68	37	±0.28	-0.32	36	±0.57	0.68	35.465	±0.81	0.535	36.09	±0.28	-0.09
I	35.19	35.35	±0.07	-0.16	36	±0.14	-0.81	34.75	±0.76	1.25	35.63	±0.49	0.37
LC	35.1	36.5	±0	-1.4	36.55	±0.92	-1.45	35.715	±1.11	0.835	37.12	±0.65	-0.57
LP2	17.28	17.15	±0.35	0.13	17.5	±0.14	-0.22	16.695	±0.08	0.805	17.14	±0.16	0.36
LM1	23.29	23.35	±0.92	-0.06	23.25	±0.07	0.04	23.26	±0.47	-0.01	23.395	±0.47	-0.145
LM2	22.78	23.45	±0.78	-0.67	22	±0.71	0.78	22.315	±0.21	-0.315	22.585	±0.16	-0.585

Table 10: Caliper vs. 4.0mA and 300 Voxel at Different locations in Mandible 2 (Distance measured in mm)

Location	Caliper	4mA 300Voxel DTX	SD±	Difference	4mA 300Voxel coD	SD±	Difference	4mA 300Voxel BSP	SD±	Difference	4mA 300Voxel SM	SD±	Difference
RM2	13.73	13.25	±1.06	0.48	13.85	±0.07	-0.12	13.285	±0.21	0.445	13.205	±0.71	0.525
RM1	13.22	13.5	±0	-0.28	13.25	±0.07	-0.03	13.655	±0.15	-0.435	13.48	±0.38	-0.26
RP2	13.72	13.9	±0.28	-0.18	13.5	±0.28	0.22	14.175	±0.21	-0.455	13.55	±0.37	0.17
RP1	12.58	12.3	±0.28	0.28	13.1	±0.14	-0.52	12.865	±0.71	-0.285	12.605	±0.81	-0.025
RC	26.51	25.8	±0.14	0.71	26.05	±0.07	0.46	25.78	±0.24	0.73	26.01	±0.59	0.5
LC	28.12	28.35	±0.07	-0.23	28.3	±0.14	-0.18	27.31	±0.72	0.81	28.415	±0.19	-0.295
LP1	10.32	9.85	±0.35	0.47	9.95	±0.64	0.37	9.335	±0.52	0.985	9.515	±0.59	0.805
LP2	13.91	14.2	±0.42	-0.29	14.55	±0.92	-0.64	14.595	±0.02	-0.685	14.08	±0.72	-0.17
LM1	14.36	13.3	±0.57	1.06	13.95	±0.78	0.41	14.31	±0.37	0.05	13.455	±0.35	0.905
LM2	13.12	12.85	±0.64	0.27	13.05	±0.35	0.07	13.22	±0.61	-0.1	13.25	±0.45	-0.13

The results of the caliper and the different anatomical locations are listed in the Table 9 and 10 for Mandible 1 and Mandible 2 respective where the CBCT parameters are set at 4.0mA with 300 Voxel. Statistically significant differences were noted in DTX at RM1 and LC for -.06mm and -1.4mm respectively. No other significant differences were observed in coD, BSP, and SM in Mandible 1. In Mandible 2, statistically significant differences were noted at RM1 in DTX for -0.28mm and at LP2 in BSP for 0.685mm. No statistically significant differences were observed in coD and SM in Mandible 2.

In Mandible 1, only 3 out the of the 36 mean values had a difference greater than 1mm. In Mandible 2, no mean values had a difference greater than 1mm. These values are highlighted in purple

3.2.6 Caliper vs. 5mA 300 Voxel

Table 11: Caliper vs. 5.0mA and 300 Voxel at Different locations in Mandible 1 (Distance measured in mm)

Location	Caliper	5mA 300Voxel DTX	SD±	Difference	5mA 300Voxel coD	SD±	Difference	5mA 300Voxel BSP	SD±	Difference	5mA 300Voxel SP	SD±	Difference
RM2	21.23	22	±0	-0.77	22.45	±1.06	-1.22	21.485	±0.69	-0.255	21.745	±0.73	-0.515
RM1	22.54	23	±0.42	-0.46	22.1	±0.57	0.44	22.66	±0.03	-0.12	22.655	±0.57	-0.115
RP2	16.5	15.55	±0.64	0.95	16.8	±0.28	-0.3	15.51	±0.55	0.99	15.985	±0.05	0.515
RC	36.68	36.1	±1.13	0.58	35.2	±1.27	1.48	35.235	±0.45	1.445	35.5	±0.44	1.18
I	35.19	34.65	±0.07	0.54	34.95	±0.64	0.24	34.54	±1.13	0.65	35.085	±0.73	0.105
LC	35.1	37.05	±0.21	-1.95	35.8	±1.13	-0.7	35.97	±0.78	-0.87	36.795	±0.45	-1.695
LP2	17.28	17.2	±0.57	0.08	17.1	±0.14	0.18	16.68	±0.11	0.6	17.09	±0.47	0.19
LM1	23.29	23.25	±0.07	0.04	23.45	±0.07	-0.16	23.11	±0.38	0.18	23.07	±0.21	0.22
LM2	22.78	23.05	±0.21	-0.27	23.35	±0.64	-0.57	22.715	±0.5	0.065	22.99	±0.83	-0.21

Table 12: Caliper vs. 5.0mA and 300 Voxel at Different locations in Mandible 2 (Distance measured in mm)

Location	Caliper	5mA 300Voxel DTX	SD±	Difference	5mA 300Voxel coD	SD±	Difference	5mA 300Voxel BSP	SD±	Difference	5mA 300Voxel SM	SD±	Difference
RM2	13.73	13.85	±0.64	-0.12	13.65	±0.07	0.08	13.11	±0.93	0.62	13.055	±0.77	0.675
RM1	13.22	13.2	±0.99	0.02	13.65	±0.21	-0.43	13.34	±0.61	-0.12	13.175	±0.28	0.045
RP2	13.72	13.45	±0.07	0.27	14.05	±0.64	-0.33	13.39	±0.28	0.33	13.61	±0.07	0.11
RP1	12.58	12.4	±0.14	0.18	12.8	±0	-0.22	12.75	±0.34	-0.17	12.5	±0.11	0.08
RC	26.51	26	±0.28	0.51	25.7	±0.28	0.81	25.675	±0.39	0.835	26.175	±0.35	0.335
LC	28.12	28.15	±0.21	-0.03	28.55	±0.35	-0.43	27.24	±0.35	0.88	28.63	±0.06	-0.51
LP1	10.32	9.95	±0.21	0.37	9.85	±0.07	0.47	9.14	±0.07	1.18	9.935	±0.56	0.385
LP2	13.91	13.8	±0.28	0.11	14.35	±0.49	-0.44	13.915	±0.86	-0.005	13.615	±0.06	0.295
LM1	14.36	13.55	±0.78	0.81	13.25	±0.07	1.11	14.03	±1	0.33	13.185	±0.28	1.175
LM2	13.12	13.6	±0.14	-0.48	13.25	±0.07	-0.13	13.71	±0.06	-0.59	12.86	±0.61	0.26

The results of the caliper and the different anatomical locations are listed in the Table 11 and 12 for Mandible 1 and Mandible 2 respectively where the CBCT parameters are set at 5.0mA with 300 Voxel. No statistically significant differences were observed in Mandible 1 in any of the softwares. In Mandible 2, statistically significant differences were noted at LP1 in SBP for 1.18mm and at LM1 in coD for 1.11mm. No statistically significant differences were observed in DTX and SM in Mandible 2.

In Mandible 1, only 5 out the of the 36 mean values had a difference greater than 1mm. In Mandible 2, only 2 out of the 40 mean values had a difference greater than 1mm. These values are highlighted in purple

3.3 Mean measurements for softwares and mean difference from caliper in Mandible 1

Mean Measurements (mm) and Mean difference from caliper in Mandible 1					
	Caliper	**DTX**	**coD**	**BSP**	**SM**
Mean	25.62	25.91	25.77	25.4	25.74
Std. Deviation	±7.896	±8.187	±8.032	±7.931	±8.185
Std. Error of Mean	2.632	2.729	2.677	2.644	2.728
Mean Difference (±SD)		-0.285 (±0.312)	-0.152 (±0.350)	0.224 (±0.246)	-0.115 (±0.312)

Table 13: Mean measurements for softwares and mean difference (in mm) from calipers for each software in Mandible 1

One-way ANOVA was used to determine the mean values and mean difference for each of the four softwares compared to the caliper measurements. ANOVA analysis attached in appendix C displayed no statistical difference between the caliper and the four softwares. Estimated Marginal means for each location is listed in table 14. All of the mean values are within the 95% confidence interval. Boxplot of the average mean values for each section corresponding to mA and voxel sizes are demonstrated in Figure 24.

Estimated Marginal Means

Grand Mean

Dependent Variable	Mean	Std. Error	95% Confidence Interval	
			Lower Bound	Upper Bound
RM2	22.145	.082	21.980	22.311
RM1	22.436	.069	22.296	22.576
RP2	16.022	.092	15.835	16.209
RC	35.985	.106	35.769	36.201
LC	36.449	.086	36.273	36.624
LP2	16.952	.074	16.802	17.102
LM1	23.413	.069	23.272	23.553
LM2	22.595	.063	22.468	22.722
I	35.328	.074	35.178	35.479

Table 14: The estimated marginal means of the first and second reading at the corresponding sections for four softwares

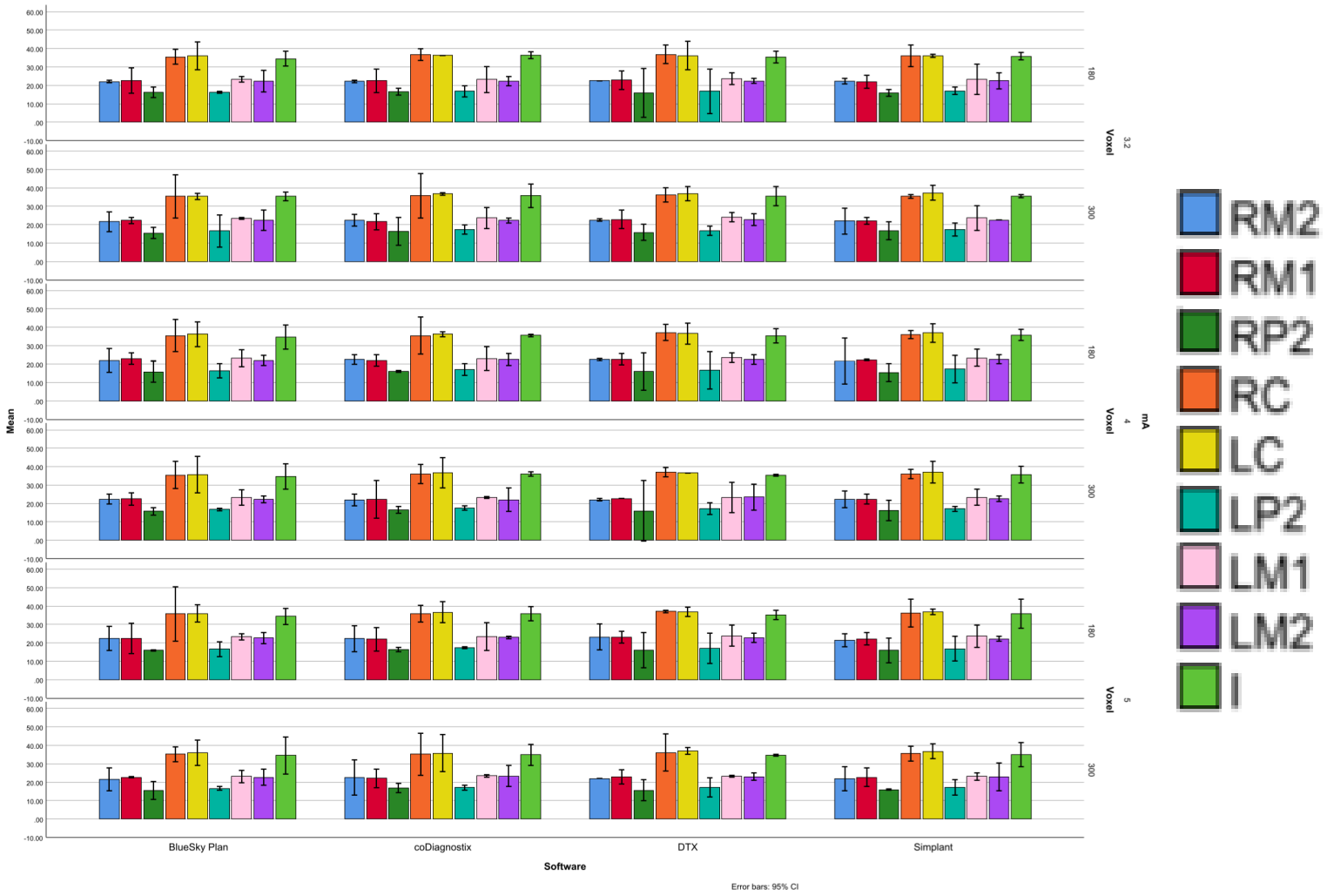

Figure 24: The average distance measured in each software for each section corresponding to mA and voxel sizes in Mandible

1

3.4 Mean measurements for softwares and mean difference from caliper in Mandible 2

Mean measurements (in mm) and mean difference from caliper in Mandible 2					
	Caliper	DTX	coD	BSP	SM
Mean	15.96	15.8	15.93	15.73	15.67
Std. Deviation	±6.099	±6.08	±6.017	±5.848	±6.155
Std. Error of Mean	1.929	1.923	1.903	1.849	1.946
Mean Difference (±SD)		0.158 (±0.269)	0.033 (±0.227)	0.226 (±0.303)	0.286 (±0.230)

Table 15: Mean measurements for softwares and mean difference (in mm) from calipers for each software in Mandible 2

One-way ANOVA was used to determine the mean values and mean difference for each of the four softwares compared to the caliper measurements in mandible 2. ANOVA analysis attached in appendix C displayed no statistical difference when comparing the means for each software and the caliper. Boxplot of the average mean values for each section corresponding to mA and voxel sizes are demonstrated in Figure 25.

3.5 Comparing Mandible 1 and Mandible 2

Mean difference (in mm) from caliper for Mandible 1 and 2 and ± SD		
Softwares	Mandible 1	Mandible2
DTX	-0.285 ±0.312	0.158 ±0.269
coD	-0.150 ±0.350	0.033 ±0.227
BSP	0.224 ±0.246	0.226 ±0.303
SM	-0.115 ±0.312	0.286 ±0.230

Table 16: Mean difference (in mm) from caliper for Mandible 1 and 2 and ± SD

Mean difference for each softwares in Mandible 1 and 2 is demonstrated in table 16. Neither of the mean differences were statistically significant when compared to their corresponding caliper readings. When comparing one mandible to another in the same software, not a single software reaches a measurement difference of 0.5mm. Paired t-tests (attached in Appendix E) were run to affirm whether a difference existed between Mandible 1 and Mandible 2. No significant difference was noted between the two mandibles used in our study.

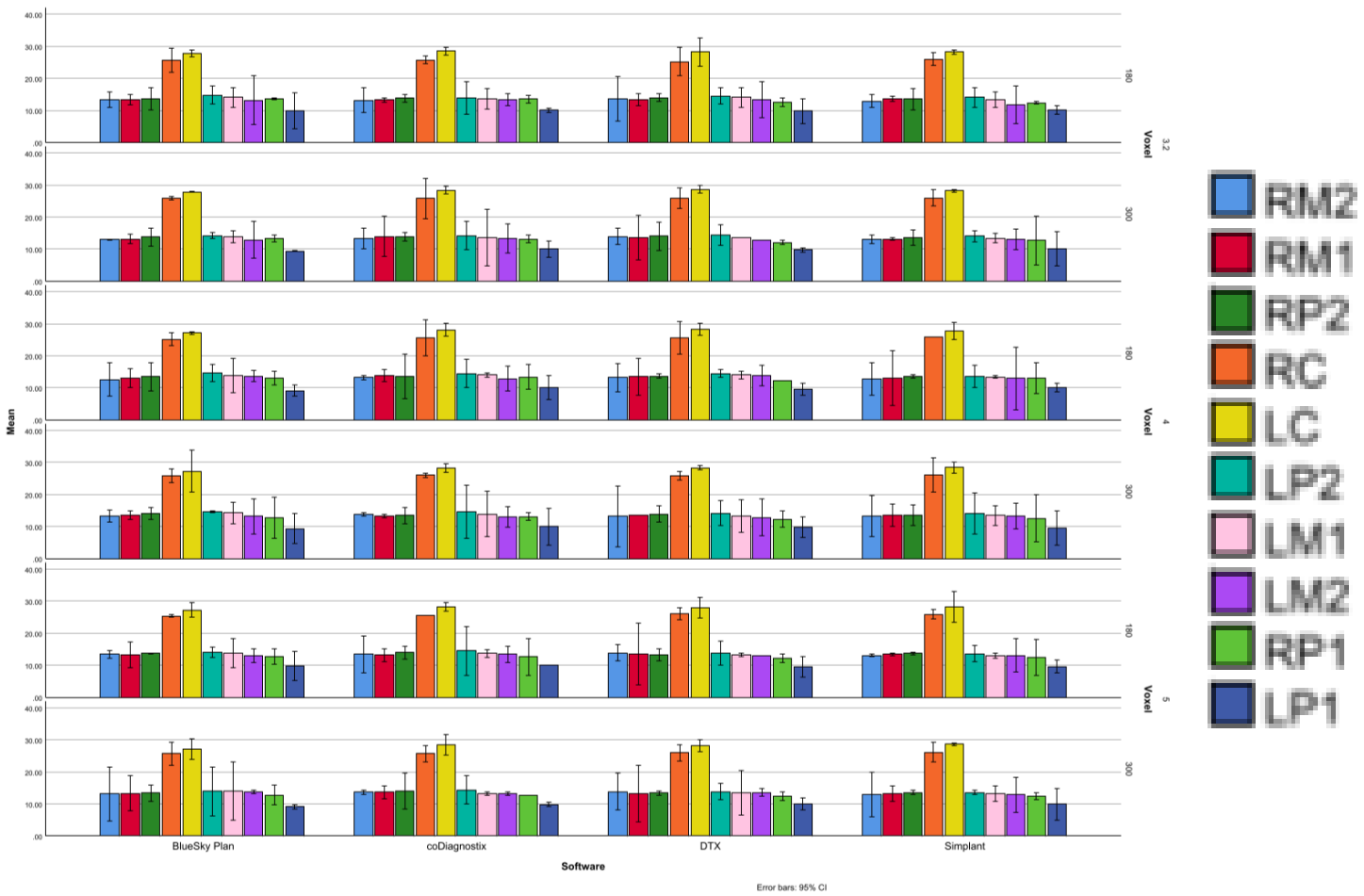

Figure 25: The average distance measured in each software for each section corresponding to mA and voxel sizes in Mandible 2

3.6 Assessing the accuracy of the software

3.6.1 Accuracy formulation and figures

In our study, to assess accuracy, relative distance measurement to the caliper or gold standard is introduced. Accuracy is defined by the value of the selected measurement which is verified as close to the true value as much as possible (Brunette, 2007). To assess the accuracy of the selected sections, a relative distance is introduced to represent the accuracy. The relative distance or measurement can be calculated from the formula:

$$\text{Accuracy} = 1 - (E - O)/\ E$$

where E is the gold standard value and O is the observed distance from software. In general, the accuracy is a number smaller or equal to 1. If the real distance and the observed distance is close, the accuracy is high (i.e., close to 1). If the observed distance is quite different from the real distance, the accuracy is low (i.e., much smaller than 1), and it may turn negative eventually.

Figure 23 shows the accuracy distribution, which is skewed left. The accuracy has minimum 0.86, maximum 1, median 0.98, mean 0.97, and standard deviation 0.024.

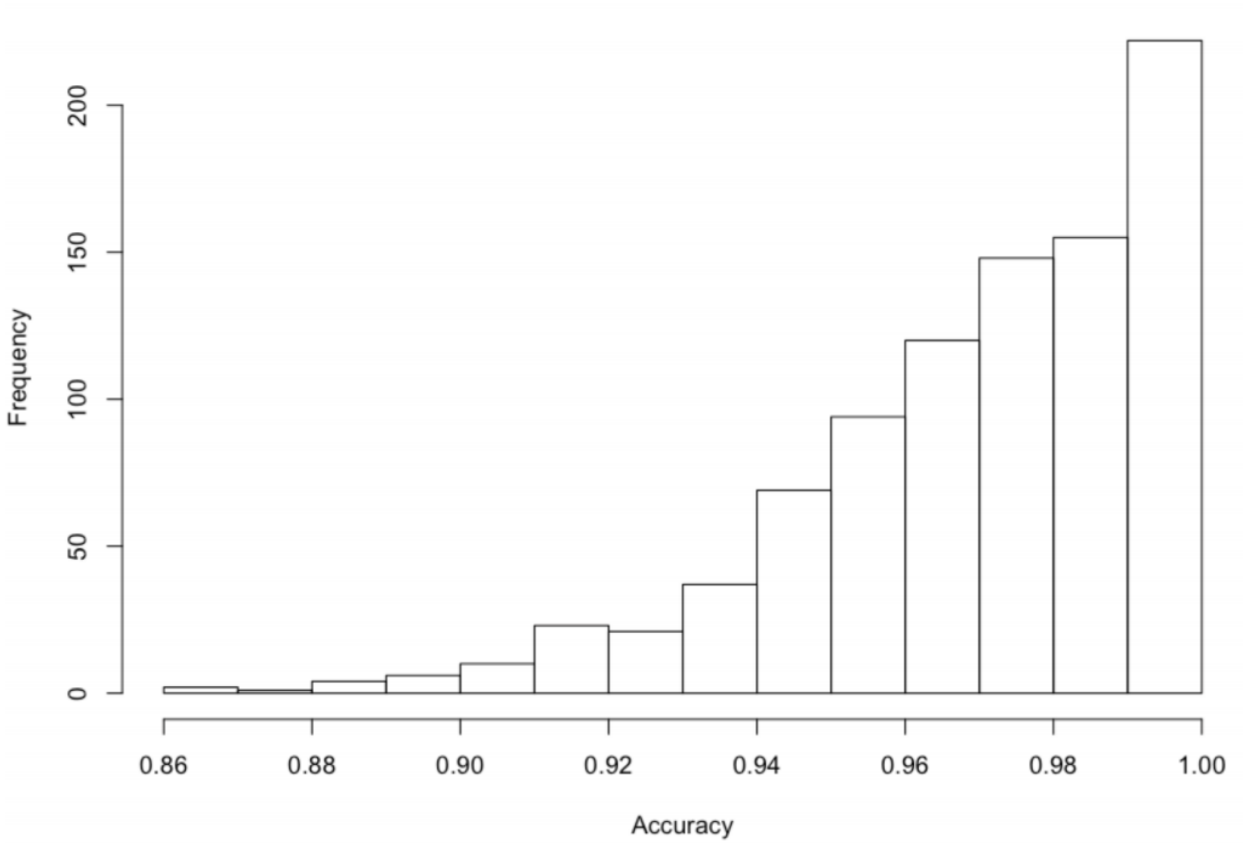

Figure 26: Histogram of accuracy distribution

Figure 27 shows a boxplot of accuracy by software, color lines by mA and each plot is subdivided by voxel sizes. Figure 28 and 29 represent the boxplot of accuracy separated by each software in Mandible 1 and 2, respectively. Figure 27, 28 and 29 do not show a big difference in accuracy among the different softwares. For location, LC appears to exhibit the lowest accuracy among most of the softwares in Mandible 1. In Mandible 2, LM1 and LPI appear to exhibit the lowest accuracy among the softwares in Mandible 2. The boxplot as shown in figures 27, 28, and 29 provide us with a superficial insight, and a statistical model is needed to confirm the primary conclusions from the plot.

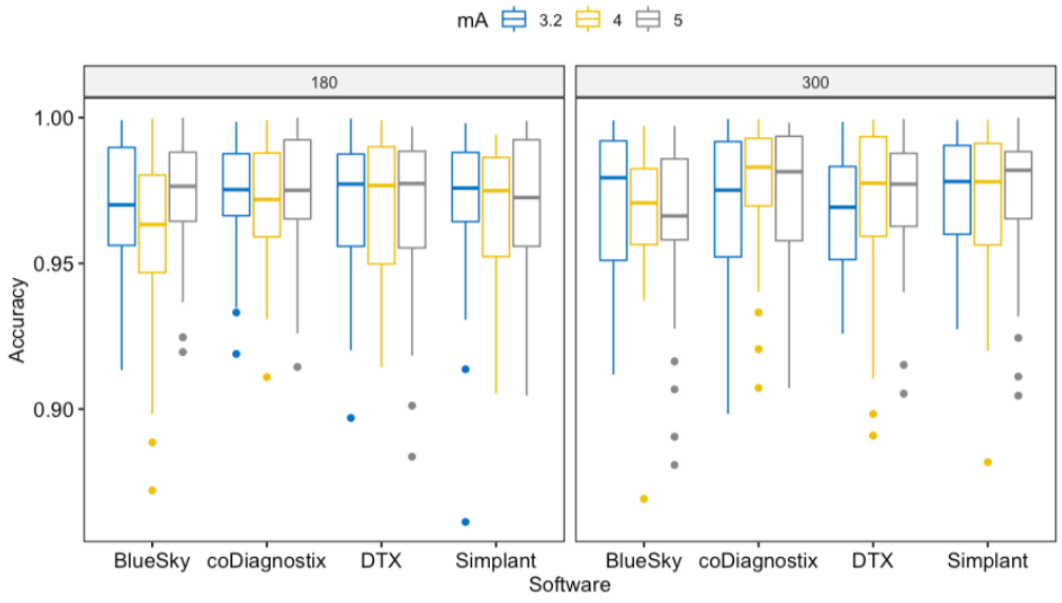

Figure 27: Boxplot of accuracy with respect to different softwares, mA and voxel sizes.

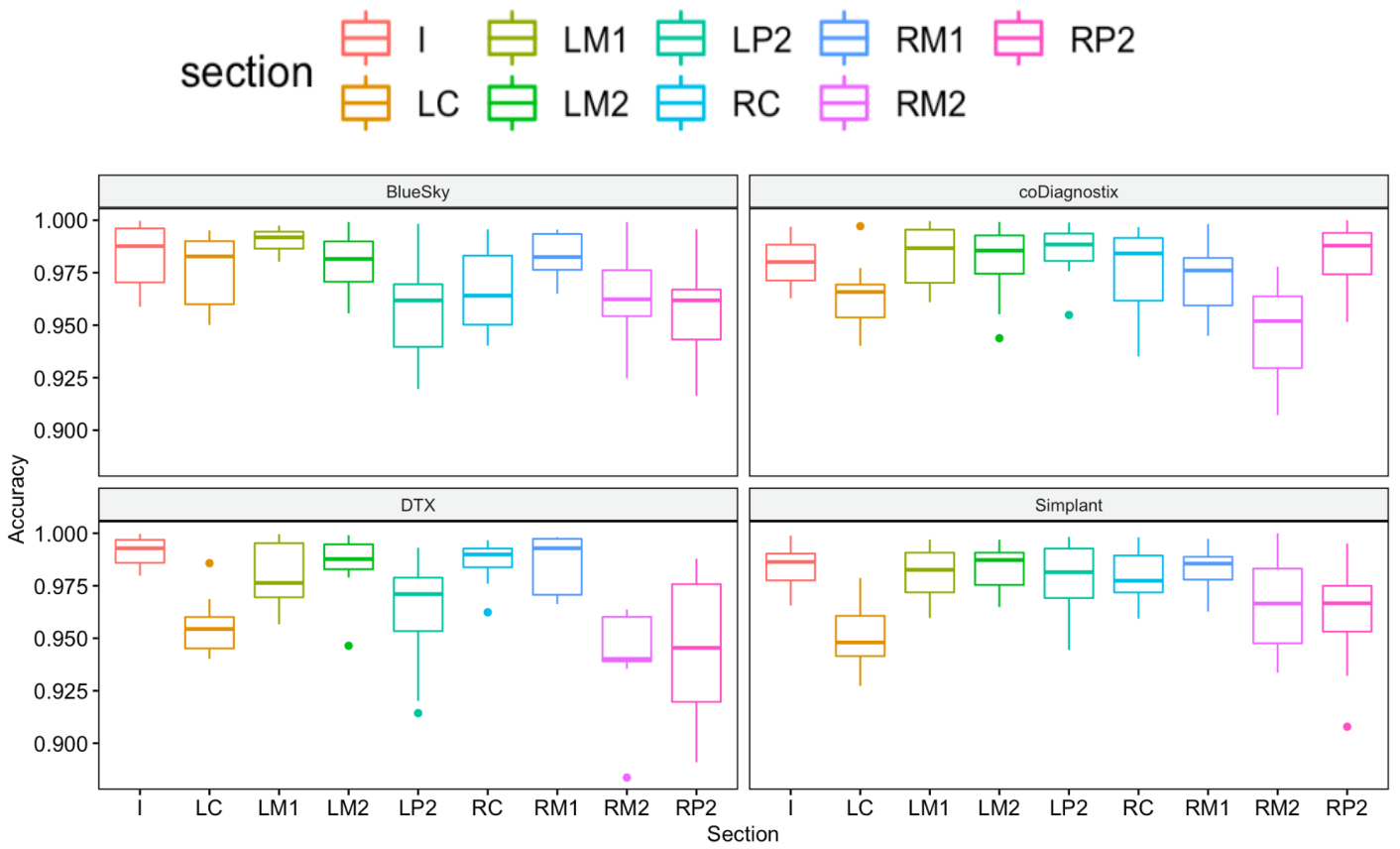

Figure 28: Boxplot of accuracy of different softwares for Mandible 1

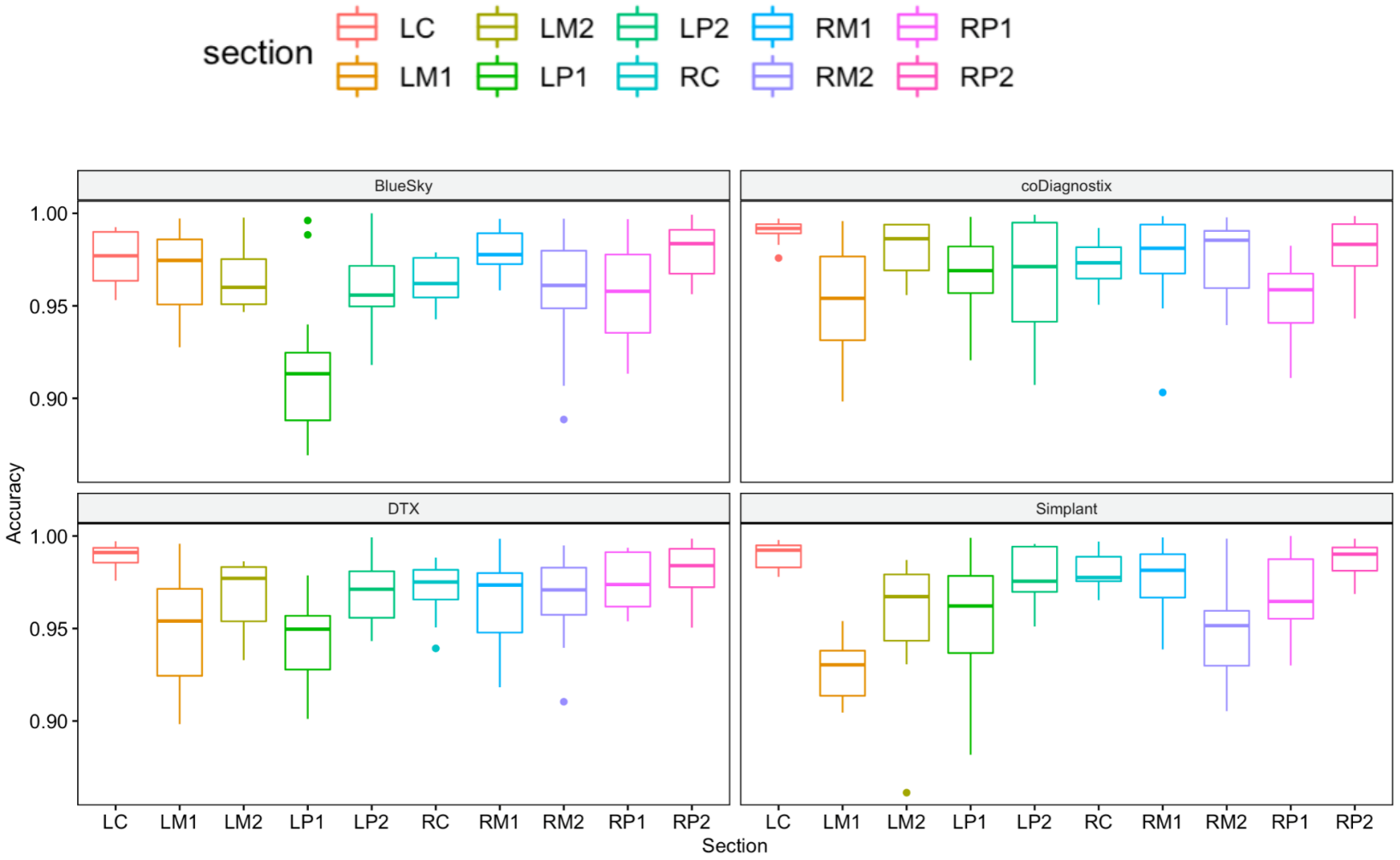

Figure 29: Boxplot of Accuracy of different softwares for Mandible 2

3.6.2 Comparing accuracy of the four implant softwares

ANOVA is used to compare the mean of multiple groups (Brunette, 2007). There are 3 grouping variables (software, mA, and voxel sizes) that can have effect on the accuracy, so a three-way ANOVA can be used to evaluate the effect of these different grouping variables on the continuous outcome variable (accuracy). This test can also be used to evaluate if there is a statistically significant interaction between these variables in explaining the accuracy. Mandible 1 has 9 different sections and Mandible 2 has 10 different sections and each section has two measurements. At each section, there are two readings for each combination of grouping variables. Since our primary interest was not to assess the effect of the section on the accuracy, it was treated as a blocking factor in three-way ANOVA analysis.

Three-way ANOVA was carried out on the data for accuracy values. The summary of the ANOVA results is displayed in Table 17. There appears to be no significant difference between the gold standard and the softwares. When comparing one software to another, the ANOVA analysis shows that there is a significant software effect at significance level of 0.05 ($p = 0.04$), i.e., at least one software has different accuracy from other software after adjusting the section effect and time effect. Furthermore, the blocking of section appears to be effective, since p-value is very small ($p < 0.01$). This suggests that value of one of the sections may not be highly accurate.

Post-hoc tests can be used to perform multiple pairwise comparison between groups. In this analysis, Tukey's Honest Significant Difference (Tukey's HSD) was used. Tukey's HSD provides with an estimate of difference between the softwares and a confidence interval for the estimate as highlighted in Table 18. The table showcases that only significant difference is

noted between coD and BSP ($p = 0.02$), and BSP has about 0.006 lower accuracy than coD. Low accuracy may due to intra-examiner variability or low reliability of the software.

	df	Sum of Squared	Mean Squared	F value	*p*-value
Section	18	0.1272	0.0071	15.269	<2e-16
Reading	1	<0.0001	<0.0001	0.006	0.940
Software	3	0.0038	0.0013	2.760	0.041
mA	2	0.0009	0.0005	1.019	0.361
Voxel	1	0.0004	0.0004	0.967	0.326
Software:mA	6	0.0022	0.0004	0.805	0.566
Software:Voxel	3	0.0006	0.0004	0.444	0.722
mA:Voxel	2	0.0014	0.0007	1.558	0.211
Software:mA:Voxel	6	0.0033	0.0005	1.174	0.318
Residuals	869	0.4021	0.0005		

Table 17: Summary of the ANOVA for accuracy

group1	group2	estimate	lower bound	higher bound	p-value
BlueSky	coDiagnostix	0.006	0.001	0.011	0.025
BlueSky	DTX	0.002	-0.003	0.008	0.645
BlueSky	Simplant	0.003	-0.002	0.009	0.318
coDiagnostix	DTX	-0.003	-0.009	0.002	0.349
coDiagnostix	Simplant	-0.002	-0.007	0.003	0.681
DTX	Simplant	0.001	-0.004	0.006	0.949

Table 18: Summary of Post-hoc tests

3.6.3 Intra-examiner variability

In addition to ICC, intra-examiner variability was also assessed to ensure high reliability of the examiner.

Intra-examiner variability can be assessed by the standard deviation of the first and second reading at each section. Figure 30 shows a boxplot of standard deviation of accuracy by software, color lines by mA and each plot is sub-divided by voxel sizes. The figure does not demonstrate a statistical difference in the figure.

A separate three-way ANOVA on the standard deviation of accuracy with 3 grouping variables (mA, voxel size and software) and one block factor (i.e., section) is performed. Table 19 shows the ANOVA results, and there are no significant differences between different types of software at significance level of 0.05, after adjusting for the blocking factor i.e. section. The results demonstrate that the intra-examiner variability is independent from different softwares but may depend on particular sections. This illustrates that certain low accuracies noted may be due to the location/section rather than the software. Adjusting for sections effect and ANOVA analysis for standard deviation of accuracy, intra-examiner variability does not appear to have a statistically significant impact on accuracy.

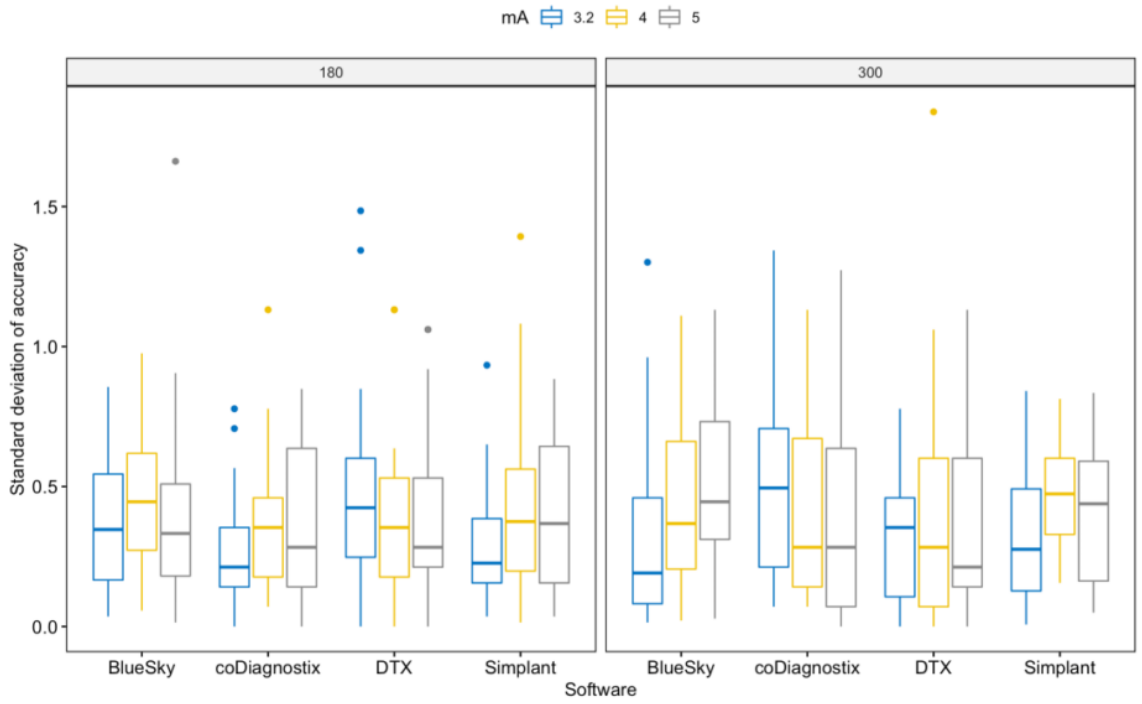

Figure 30: Boxplot of Standard deviation distribution of accuracy by software, mA and voxel sizes

	df	Sum of Squared	Mean Squared	F value	p-value
Section	18	5.076	0.282	3.078	2.63e-05
Software	3	0.045	0.015	0.162	0.922
mA	2	0.310	0.155	1.690	0.186
Voxel	1	0.009	0.009	0.095	0.759
Software:mA	6	0.352	0.059	0.640	0.699
Software:Voxel	3	0.375	0.125	1.365	0.253
mA:Voxel	2	0.013	0.007	0.072	0.931
Software:mA:Voxel	6	0.551	0.092	1.002	0.423
Residuals	414	37.922	0.092		

Table 19: Summary of the ANOVA for intra-examiner variability

3.6.4 Sensitivity

Specificity, sensitivity, positive and negative predictive values are common terms noted in medical nomenclature and diagnosis. These statistical values help in determining the

likelihood of disease or health in a given population. In this study, these terms cannot be applied directly as the outcome of our study is not binary i.e. accuracy is being given as continuous probability outcome. In such scenario, sensitivity can be assessed by choosing a threshold *T* (value) of accuracy. A clinically significant threshold, *T*, is chosen, and measurements with accuracies greater than *T* from the gold standard are deemed adequate or sufficient. The proportion of measurements which are considered accurate for different threshold values can then be assessed. While this is not consistent with the definition of any of the sensitivity, specificity, PPV or NPV, it is similar in idea to these measures while being applied to the context of this study.

Assume that the observed measurement is accurate if the corresponding accuracy is above the threshold T. Sensitivity depends on the threshold T and it is summarized in Table 20. Table 20 shows that coDiagnostix has the highest sensitivity compared to other software.

	Threshold T	0.93	0.94	0.95	0.96	0.97	0.98	0.99
Sensitivity	BlueSky	0.90	0.86	0.79	0.65	0.51	0.36	0.20
	coDiagnostix	0.94	0.91	0.83	0.74	0.61	0.44	0.30
	DTX	0.92	0.88	0.78	0.70	0.57	0.41	0.24
	Simplant	0.93	0.87	0.82	0.73	0.61	0.43	0.24

Table 20: Sensitivity for different threshold values for different softwares

3.7 Location

Two-way ANOVA was also carried out which affirms that biggest variation in accuracy is due to different locations/sections rather than the different softwares, mA and voxel sizes. Results from the Two-way ANOVA are listed in Appendix D.

Measurement values that demonstrated a statistically significant differences were noted at RM2, RM1, and LC. RM1 only had 1 out of 24 measurements that showed a statistically significant difference while RM1 and LC had 2 and 3 out of 24 measured values, respectively that showed a statically significant difference.

Measurement values that demonstrated statistically significant differences were noted at RM2, RM1, RP1, RC, LP1, LP2, LM1, and LM2 in Mandible 2. Only 1 out the 24 measured values that showed a statistically significant difference was noted at RM2, RM1, LP2 and LM1 in Mandible 2. In Mandible 2, two or more of the readings that showed statistical significance were noted at RP1 (3 out of 24 measured values), RC (3 out of 24 measured values), LP1 (2 out of 24 measured values), and LM2 (2 out 24 measured values).

Chapter 4: Discussion

Until the advents of CBCT, dental panoramic radiographs have been the staple in imaging anatomical landmarks. Over the last two decades, CBCT has become more widely used in dentistry more specifically the planning and placement of dental implants. The advantages of being able to identify anatomical landmarks is a significant advantage. The software viewing packages included in the study as they represent the biggest global market shares in dental implants (iData research 2021). coD, DTX and SM can cost thousands of dollars to purchase with a subsequent subscription fee for maintenance. BSP was chosen as it is a freeware software to provide a comparison and see if it may be a viable alternative. Currently, there has been no set standard for CBCT scan parameters. Furthermore, there has been minimal studies on the softwares utilized to view these scans and their accuracy. This study attempted to answer both matters presented and provide valuable feedback. Overall, the distribution of the entire data (Figure 26) is highly accurate and similar to prior studies conducted for linear accuracy (Fokas et al. 2018). According to our results, there was no statistical significance between the softwares and the caliper measurements. When comparing one software to another, only significant difference was noted between coD and BSP. BSP yielded a 0.006 accuracy rating lower than coD. Although statistically significant, it only represents 0.6% of measurement difference from coD. When computing this in for mean measurement value for the softwares even when taking the biggest difference in Mandible 1 the difference would yield 0.02mm on average (calculation in Appendix D). It is not possible to see this value being clinically relevant. This was also reflected in the sensitivity values that were calculated where coD had the highest sensitivity among the softwares.

Previous studies (Fokas et al. 2018, Kobayahsi et al. 2004) have noted that for CBCT measurements to be deemed clinically relevant, the discrepancy between the gold standard and the measurement should be 1 mm or less. All of the mean values for each of the softwares were within this range. Out of 456 measurements, 410 measurements were within this range. While this provides a good overall view, it must be noted that this also includes certain locations and measurements which may show high variability and may not truly represent the reliability and accuracy of the softwares. Furthermore, the 1mm difference in measurement can signify a high variability in accuracy as the difference will be significant larger for a shorter distance than a larger distance. For example a 1mm difference at RM2 in Mandible 2 in our study will be noted to be a 92% ((12.73/13.73) x100%) and 1mm difference at RM2 in Mandible 1 in our study will be noted to be 95% ((20.23/21.23) x 100%)). This highlights the fact that an arbitrary 1mm difference can be variable for different distances. Therefore, the accuracy equation/model used in our study provides a context to the raw numbers and differences observed in our study. Our results noted that the overall mean accuracy is 0.97 with a median value of 0.98. These figures are similar to the values observed by Watrick et al. (2013) where they also noted a similarly high agreement between CBCT measurements and digital calipers. Furthermore, for implant planning, the safety zone of 2mm has been proposed by Greenstein and Tarnow (2006). The grand means of both Mandible 1 and Mandible 2 are within this range for our study.

4.1 Caliper vs. mA.

mA represents the dose that is generated by the tube current (Pauwels et al. 2015). Due to CBCT generally having a functional mA that are usually under one order of magnitude of medical CT machines, a higher noise level is projected in CBCT images (Schulze et al. 2011).

Noise is a result of additional measured x-ray attenuation that is non-linear and contributes to image degradation (White and Pharoah, pg. 236). A method to reduce noise is by increasing mA however that comes at the cost of subsequent increase in radiation dose (Pauwels et al. 2015). Our study found no significant impact of different mA values (3.2, 4.0, and 5.0) on the accuracy of softwares. The results are in alignment with Kim et al. (2010) where the authors compared the CBCT to the direct measurement in measuring the mandibular canal. These authors used mA ranging from 3.0 to 8.0 and 0.2 voxel sizes. Their study found no significant differences between the CBCT measurements at different mA values and direct measurements. The study utilized the iCat CBCT which also has a 180-degree rotation similar to the CBCT machine used in current study. Furthermore, the results are further affirmed by Hans et al. (2020) where the biggest discrepancy between linear measurements on the CBCT were found between 2mA and 10mA by using the same CBCT machine.

Although the image quality was not quantitively assessed in current study, there was no apparent scanning parameter that made it challenging to assess the anatomy or the measurement of the scan. Similar findings are noted by Sur et al. (2010) where they noted that there was no significant impact on image quality between 4mA and 8mA in regard to implant planning. The authors noted that scans taken at 2mA and 360 degrees and 4mA and 180 degrees all produced sufficient image quality. These are also affirmed by Dawood et al. (2012) where by images were graded from 2mA to 6mA and no significant impact on image quality was noted for implant planning.

4.2 Caliper vs. Voxel size

Our study found no significant impact of different voxel sizes (0.18mm and 0.30mm) on the accuracy of softwares. Waltrick et al. (2012) also studied the effects of varying voxel sizes on the visibility of the mandibular canal and it's accuracy in linear measurements. The study utilized gutta percha markers in the buccal and lingual aspects similar to the ones used in current study and linear measurement corresponding to different cross sections. In contrast to our study, Waltrick et al. (2012) only utilized three preset points in the proximity of second molar, first molar and second premolar. In addition, they only used edentulous mandible. The different voxel size analyzed were 0.2mm, 0.3mm and 0.4mm. They noted that voxel size did not impact accuracy from linear measurement except of linear accuracy at first molar. They also noted that voxel size of 0.2mm produced the best visible image while 0.3mm may be the best compromise between 0.2 and 0.4mm as to avoid increase in radiation dose with 0.2mm. It must also be noted that in their study while the kVp was kept constant at 120 kVp, the mA values ranged from 3 to 8 mA. The authors did not mention whether different mA values had an impact on their results. Similar results are obtained by Damstra et al. (2010) where the authors also compared linear measurements to the preset gutta markers and noted no significant different between 0.2mm and 0.4mm. It must be noted that the authors used SimPlant Ortho to view the CBCT images. The SimPlant Ortho software is manufactured by the Dentsply Sirona corporation and maybe similar to the software used in our study. The results of our study are comparable to the results of Damstra et al. (2010) where we can corroborate the voxel sizes do not impact CBCT images viewed in Simplant. Patcas et al. (2012) also found no significant impact when using 0.125mm and 0.4mm voxel sizes to compare the accuracy of CBCT when

assessing bone overlying teeth in the anterior mandible. Furthermore, it was observed that even with .125mm voxel size, alveolar buccal plate which tends to be extremely thin could not be consistently identified. Therefore, it may be an extreme to take a CBCT image in that particularly small voxel settings which increase a significant radiation dose to the patient.

4.3 Variation at locations

When reviewing ANOVA analysis, the biggest variation of results was noted to be due to location/section. In our current study, the biggest variation and the lowest accuracy is noted at LC in Mandible 1 as noted by the accuracy tables and the Dunnet's multiple comparison test as seen in Appendix D. This may be due to the cortication of the trabecular bone in the most superior aspect where I made the measurements. As noted by the Patcas et al. (2012) even at .12mm voxel size, thin cortical plate is not accurately assessed in the anterior mandible and trabecular bone tends to be significantly less dense than cortical plate. It must also be noted that while it is the least accurate area, only 3 mean measurement values out of 24 showed a statistically significant difference. Two of those values do arise from the higher voxel size value of 0.3mm viewed in coD and DTX. It is more plausible that due to high intra-correlation coefficient (ICC) and the inaccuracy reproducing itself more often that I may have misinterpreted the landmark in the software measurement in comparison to the caliper measurements.

While Mandible 2 demonstrated the greatest number of locations with statistically significant differences, the lowest to highest range of difference in all of the sections were within the gold standard difference of 1mm or less with the exception of 3 readings where the underestimation of 1.3mm was noted at RC, LM1, LM2. The lowest accuracy and the biggest

variation in Mandible 2 were noted to be RP1, RC, LP1, LM1. It must be noted that there were only 3 and 2 mean measurement values out of 24 for RP1, RC and LP1, LM1 respectively, that showed a statistical significant difference as per two-way ANOVA analysis which is attached in Appendix D. The statistically significant differences in ANOVA were seen at RP1 measurements done 3.2 mA/0.18mm voxel (BSP), 5mA/0.30mm voxel (coD), 4 mA/0.18mm voxel (DTX). The minimum and the maximum range of difference noted at RP1 is -1.07mm to 0.53mm. It is interesting that the highest inaccuracies also resulted in the LP1 position on the contralateral side. The statistically significant differences as per Two-way ANOVA (Appendix D) were seen at LP1 in scans at 5mA/0.18mm voxel (coD) and 3.2mA/0.30 voxel (BSP). The ranges of mean differences noted at LP1 were from -0.18mm to 1.185mm. The inaccuracy noted could be due to the decreased visibility of the cortex of the mandibular canal. Ishii et al. (2018) noted that the superior aspect of the mandibular canal tended to decrease in visibility as you move from posterior to the anterior. They noted the lowest visibility of the superior cortex was the lowest in the area of the mental foramen and the highest towards the second molar region. In their study, the authors noted that two thirds of the most superior portion of the mandibular canal could only be identified in 44% and 62% of their study population. Similar results are noted by Jung and Cho (2014) where they observed the lowest visibility of the canal in the proximity of the first molar. These results may help explain the higher number of inaccuracies noted at LM1 in Mandible 2 which was noted to be in the proximity of the first molar. The range of mean difference at LM1 in Mandible 2 is from 0.05mm to 1.305mm. Although the second molar is noted to have the highest amount of visibility of mandibular canal, Ishii et al. (2018) noted that the superior and inferior cortex of the canal can only be

visualized approximately 66% of the time. This can provide a plausible explanation of the 2 (out of 24) measurement error values noted at RM2 in this study.

At RC, statistical significant differences as per Two-way ANOVA (Appendix D) analysis were observed in measurements done in 5mA/0.18mm voxel (coD), 5mA/0.18mm voxel (BSP), and 4mA/0.18mm voxel (SM). The range of difference noted at RC was 0.335mm to 1.36mm. It appears that most of the inaccuracies resulted from 0.18mm voxel size. This is the hypothetically similar position to the inaccuracy noted at LC in Mandible 1. In contrast to Mandible 1, most of the inaccuracies in Mandible 2 at the canine position resulted from the lower voxel size 0.18mm rather than 0.30mm voxel size. Although decreasing voxel size, provides better spatial resolution, 0.18mm may not be able to capture the thin buccal plate at the anterior mandible (Patcas et al. 2012). Menezes et al. (2016) observed the accuracy of CBCT in comparison to physical anatomical measurement while varying the voxel sizes. The authors compared the distance from the crest of the CEJ to crest of the buccal plate along various landmarks including the canine. The study design was similar to the current study as the distance was measured in cross section. The authors noted a mean difference of -0.52mm, -0.91mm and -0.49mm at the canine position in 0.20mm, 0.30mm and 0.40mm voxel size respectively. The mean difference of the statistically significant values in our study at RC ranged from 0.62mm to 1.19mm. It must be noted that in contrast to the Menezes (et al. 2016) study, even though their study shows lesser ranges of differences, the authors are only comparing the distance from the CEJ to the crest which they noted to be 4.18mm in physical measurement. If the accuracy equation/model in our study is applied to their measurements, then accuracy model would yield 0.876, 0.782, and 0.882 for 0.20mm, 0.30mm and 0.40mm

voxel size respectively. These values are significantly lower than the values in the current study.

4.4 Mandible 1 and Mandible 2 (Dentate vs Edentulous)

This study used two mandibles, a dentate (Mandible 1) and an edentulous (Mandible 2) one. From mean measurement analysis (table 16) of each of the softwares at these two mandibles, it does not appear that there is a significant clinical difference, as noted by One-way ANOVA of the mean measurements highlighted in Table 16 (Chapter 3). Furthermore, paired t-tests which was used to analyze and compare the mean differences between these mandibles for each software showed no statistical difference between them. Furthermore, each data point was thoroughly examined and observed to search for pattern to observe whether there might be a possibility that the difference between them may be able to explain the minor differences noted at various locations. Two-way ANOVA (appendix D) demonstrates the most significant amount of data in respect to various locations as noted in previous section.

It must be noted that in our current study, more measurements with statistically significant value differences were noted in Mandible 2 than Mandible 1 (14 vs. 7) when looking at Two-way ANOVA analysis. These values are highlighted by the Two-way ANOVA analysis and Dunnett's multiple comparison test which are given in Appendix D. While it appears that there is more than "double" the amount of error values in Mandible 2 than Mandible 1, certain things should be remarked upon. It must be noted that there was an extra location/section marked in Mandible 2 and each location had 24 mean values assigned to it. This would translate to approximately 14 out of 240 values for Mandible 2 and 7 out of 216 equivalent values for Mandible 1. This would amount to approximately 5.8% and 3.2% values of all of the values

present in the ANOVA analysis. Furthermore, from our Two-way and Three-way ANOVA analysis, we know that mA, voxel size and softwares did not have a significant impact on accuracy therefore if we take out locations with just 1 measurement displaying a statistical significance, we are left with RC and RM2 in Mandible 1 and RP1, RC, LP1, LM2 in Mandible 2. Similar locations (canine and second molar) are observed in both mandibles and possible reasons of error in these locations were discussed in the previous section. It is interesting that the area of pre-molar and mental foramen was the area of more error values in the edentulous versus dentate area. This is contrast to Suomalainen et al. (2008) where they noted increase in measurement error in the area of mandibular left premolar in the dentate mandible as compared to the edentulous when comparing linear accuracy of CBCT to CT using cadavers. These authors attributed the error to being unable to distinguish the correct height of crestal portion in the dentate mandible compared to the edentulous mandible. These errors were likely avoided in this study as I found the dentate mandible to provide additional landmarks for sectioning. Furthermore, the dentate mandible in our study was subjectively found to have a thick cortical plate in the region. This could be a possible source of error for the edentulous mandible used in our study as a slight variation in noting the highest crestal point on scanned images can have a significant impact in comparison to the gold standard. Since the distance in these areas is relatively less than the Mandible 1 (dentate), a small difference can have a higher impact particularly combined by the fact that the visibility of the canal and the foramen tends to be lower in the proximity of premolars are noted by Ishii et al. (2018).

4.5 Method of detecting mandibular canal

It must be pointed out that in our current study to detect the mandibular canal, free hand tools provided in the software were used to accurately identify using transaxial views. Consideration was given to use the automated tool in each software to map and localize the mandibular canal however it would not reliably test the accuracy of the softwares which was our primary objective. Bahrampour et al. (2015) attempted to illustrate the automated method of detecting mandibular canal via algorithm based on image recontruction. The authors noted that the mean distance error was less than 1mm from the gold standard. It must be noted that the gold standard in their study was prior agreement of the mapping of the mandibular canal as compared to automated generated curve on the software. Further recommendations of this study would include the accuracy of the computer-generated curve to the gold standard by way of digital calipers.

The method of reproducibility utilized in the current study was tracing of the mandibular canal by utilizing reconstructed DPR's from CBCT and using axial, cross-sectional and sagittal views to mark it. Gerlach et al. (2010) tested the method of reproducibility of tracing the mandibular canal by comparing reconstructed DPR images and coronal views. The authors found that the best reproducibility was achieved when the two tracing methods were combined together. They noted that the safety margin be kept at 1.7mm in all directions as they found the 95^{th} percentile deviation of 1.3mm with standard deviation of approximately 0.4mm.

4.6 Limitations

Although we try and ensure that there are no errors, some form of human error is to be expected. One of the sources for variation noted at the locations can be due to the error in

measurement. These errors can arise if a particular cross-section on the CBCT is not corresponded to the anatomical cross-sections. These could have caused the discrepancies noted at a particular section as discussed before. The challenge may have been either sectioning along with the mentioned the gutta percha points. Although permanent markers were drawn to correspond with gutta percha points, only one gutta percha marker was used on the lingual surface. A possible solution can be to use a notch to embed the gutta percha point thereby ensuring with great confidence that sections are being measured and cut at that particular section.

There was a sole observer for the current study. This was done to ensure that biases in the measurements would be as low as possible as the error in the measurements would be consistent throughout the study. We were attempting to answer the accuracy and therefore required reliability of measurements to be done to a certain extent. The use and manipulation of these software's does require certain education and skill level therefore having a person who is not familiar with all of the softwares would have a big potential to bias the results.

It is also important to mention that 2 human mandibles were used for the study. Perhaps, if a larger sample size was attainable a more pronounced difference could have been observed. The challenge in conducting this was *in vitro* study was the acquisition of human mandibles. These resources are scarcely available. Some of the previous studies have employed pig-jaws or resin to accommodate for the cortex of the bone. The advantage in that is that it does afford a large sample size however the minutiae in those studies is that it can never to truly be applicable to clinical settings. While only 2 mandibles or 4 hemi-mandibles were used, it is important to note that had over 900 data points which are in line or superior to some of

accuracy studies involving human cadavers that have been done in the past. (Neves et al. 2014, Vasconcelos et al. 2018, Fokas et al. 2018).

4.7 Future directions:

The accuracy of all four softwares was found to be remarkably high for all of the landmarks involved. It is important to note that only mandibles were used for the study. This study can be repeated to involve the maxilla and see if these values are consistent. Previous study done by Luangchana et al. (2015) found a bigger discrepancy between CBCT and anatomical measurements in the maxilla as compared to the mandible.

It is also important to note that the dentate and the edentulous mandibles used for the study had no metal objects, restorations or implants. These objects tend to introduce scatter and may end up producing a less than ideal image especially in the area of the implant planning. It is very common for patients receiving implant therapy to have direct or indirect restorations in their mouth. The parameters of this study and the softwares can be tested to see if the accuracy may change when introducing these objects. Ismail et al. (2020) found no statistically significant differences when introducing increase in metal restorations in linear accuracy. The authors noted that the softwares used in their study for implant planning (DTX and CS9300) also had no statistical difference between them. It must be noted that the study conducted was done on a pig mandible and can only be applicable to a certain extent.

Every software and the capabilities are designed to make it easier for the clinician to view and plan the case. There have been limited studies done on the level of knowledge required to operate and accurately assess important landmarks. This can be done by inviting

clinicians of various skill levels and perhaps graduate residents to see if there would be a significant impact between the level of training and accuracy.

Chapter 5: Conclusion

The goal of this study was to assess the accuracy of the four different implant planning softwares coD, DTX, Simplant and Blue Sky Plan. Linear measurements along preset points were compared to the gold standard "truth" by anatomical measurement via digital calipers. The scanning parameters of mA and voxel sizes were varied to determine if there was any impact on the accuracy of the measurements. Based on the results of the study, reserach hypothesis can be rejected.

- This study reports that there was no statistical difference between the accuracy of the softwares in measuring linear distances in human mandibles.
- Varying mA (3.2, 4.0, and 5.0) had no statistical impact on the accuracy of the softwares.
- Varying voxel sizes (0.18mm and 0.30mm) had no statistical impact on the accuracy of the softwares.
- Comparison of accuracy values between different softwares showed a statistical significance between coD and BSP. coD had a 0.006 value higher than BSP. Although statistically significant, it is not likely to be clinically significant as this does not violate the safety threshold of 1mm.
- coD, DTX, Simplant and BSP are accurate and reliable softwares in detecting the mandibular canal within the limitations of the study

Bibliography

Agthong, S., Huanmanop, T., & Chentanez, V. (2005). Anatomical variations of the supraorbital, infraorbital, and mental foramina related to gender and side. Journal of oral and maxillofacial surgery, 63(6), 800–804. https://doi.org/10.1016/j.joms.2005.02.016

Akkaya, N., Kansu, O., Kansu, H., Cagirankaya, L. B., & Arslan, U. (2006). Comparing the accuracy of panoramic and intraoral radiography in the diagnosis of proximal caries. Dento maxillo facial radiology, 35(3), 170–174. https://doi.org/10.1259/dmfr/26750940

Angelopoulos, C., Thomas, S. L., Hechler, S., Parissis, N., & Hlavacek, M. (2008). Comparison between digital panoramic radiography and cone-beam computed tomography for the identification of the mandibular canal as part of presurgical dental implant assessment. Journal of oral and maxillofacial surgery, 66(10), 2130–2135. https://doi.org/10.1016/j.joms.2008.06.021

Arai, Y., Tammisalo, E., Iwai, K., Hashimoto, K., & Shinoda, K. (1999). Development of a compact computed tomographic apparatus for dental use. Dento maxillo facial radiology, 28(4), 245–248. https://doi.org/10.1038/sj/dmfr/4600448

Bahrampour, E., Zamani, A., Kashkouli, S., Soltanimehr, E., Ghofrani Jahromi, M., & Sanaeian Pourshirazi, Z. (2016). Accuracy of software designed for automated localization of the inferior

alveolar nerve canal on cone beam CT images. Dento maxillo facial radiology, 45(2), 20150298-20150298. https://doi.org/10.1259/dmfr.20150298

Brunette, D. M. (2007). Critical Thinking : Understanding and Evaluating Dental Research: Vol. Second edition. Quintessence Publishing Company Inc.

Chan, H. L., Leong, D. J., Fu, J. H., Yeh, C. Y., Tatarakis, N., & Wang, H. L. (2010). The significance of the lingual nerve during periodontal/implant surgery. Journal of periodontology, 81(3), 372–377. https://doi.org/10.1902/jop.2009.090506

Damstra J, Fourie Z, Huddleston Slater JJ, Ren Y. (2010). Accuracy of linear measurements from cone-beam computed tomography-derived surface models of different voxel sizes. American Journal of Orthodontics and Dentofacial Orthopedics, 137(1):16.e1-6; discussion 16-7. DOI: 10.1016/j.ajodo.2009.06.016.

Dantas, J. A., Montebello Filho, A., & Campos, P. S. (2005). Computed tomography for dental implants: the influence of the gantry angle and mandibular positioning on the bone height and width. Dento maxillo facial radiology, 34(1), 9–15. https://doi.org/10.1259/dmfr/57866813

Dave, M., Coulthard, P., Patel, N., Seoudi, N., & Horner, K. (2020). Letter to the Editor: Use of Dental Radiography in the COVID-19 Pandemic. Journal of dental research, 99(9), 1112. https://doi.org/10.1177/0022034520923323

Dawood, A., Brown, J., Sauret-Jackson, V., & Purkayastha, S. (2012). Optimization of cone beam CT exposure for pre-surgical evaluation of the implant site. Dento maxillo facial radiology, 41(1), 70–74. https://doi.org/10.1259/dmfr/16421849

Denio, D., Torabinejad, M., & Bakland, L. K. (1992). Anatomical relationship of the mandibular canal to its surrounding structures in mature mandibles. Journal of endodontics, 18(4), 161-165.

Doh, R. M., Shin, S., & You, T. M. (2018). Delayed paresthesia of inferior alveolar nerve after dental surgery: case report and related pathophysiology. Journal of dental anesthesia and pain medicine, 18(3), 177–182. https://doi.org/10.17245/jdapm.2018.18.3.177

Farman A. G. (2002). There are good reasons for selecting panoramic radiography to replace the intraoral full-mouth series. Oral surgery, oral medicine, oral pathology, oral radiology, and endodontics, 94(6), 653–655. https://doi.org/10.1067/moe.2002.129766

Fishel, D., Buchner, A., Hershkowith, A., & Kaffe, I. (1976). Roentgenologic study of the mental foramen. Oral surgery, oral medicine, and oral pathology, 41(5), 682–686. https://doi.org/10.1016/0030-4220(76)90325-x

Fokas, G., Vaughn, V. M., Scarfe, W. C., & Bornstein, M. M. (2018). Accuracy of linear measurements on CBCT images related to presurgical implant treatment planning: A systematic review. Clinical oral implants research, 29 Suppl 16, 393–415. https://doi.org/10.1111/clr.13142

Gerlach, N. L., Meijer, G. J., Maal, T. J., Mulder, J., Rangel, F. A., Borstlap, W. A., & Bergé, S. J. (2010). Reproducibility of 3 different tracing methods based on cone beam computed tomography in determining the anatomical position of the mandibular canal. Journal of oral and maxillofacial surgery, 68(4), 811–817. https://doi.org/10.1016/j.joms.2009.09.059

Greenstein, G., & Tarnow, D. (2006). The mental foramen and nerve: clinical and anatomical factors related to dental implant placement: a literature review. Journal of periodontology, 77(12), 1933–1943. https://doi.org/10.1902/jop.2006.060197

Hans, A. (2020). The use of cone beam computed tomography for implant treatment planning at UBC (T). University of British Columbia. Retrieved from https://open.library.ubc.ca/collections/ubctheses/24/items/1.0392958

iData Research (2021). Dental Implants Market Analysis: United States: COVID19: 2021-2027. Accessed: Feb. 9, 21: https://idataresearch.com/product/dental-implants-market-united-states/#:~:text=Over%2050%25%20of%20the%20US,active%20in%20the%20US%20market.

Ismail, A. (2020). Measurement accuracy in cone beam computed tomography in the presence of metal artifact (T). University of British Columbia. Retrieved from https://open.library.ubc.ca/collections/ubctheses/24/items/1.0392375

Ishii, H., Tetsumura, A., Nomura, Y., Nakamura, S., Akiyama, M., & Kurabayashi, T. (2018). Diagnostic ability of limited volume cone beam computed tomography with small voxel size in identifying the superior and inferior walls of the mandibular canal. International journal of implant dentistry, 4(1), 18. https://doi.org/10.1186/s40729-018-0133-7

John, G. P., Joy, T. E., Mathew, J., & Kumar, V. R. (2015). Fundamentals of cone beam computed tomography for a prosthodontist. Journal of Indian Prosthodontic Society, 15(1), 8–13. https://doi.org/10.4103/0972-4052.157001

Jung, Y. H., & Cho, B. H. (2014). Radiographic evaluation of the course and visibility of the mandibular canal. Imaging science in dentistry, 44(4), 273–278. https://doi.org/10.5624/isd.2014.44.4.273

Kernen, F., Kramer, J., Wanner, L., Wismeijer, D., Nelson, K., & Flügge, T. (2020). A review of virtual planning software for guided implant surgery - data import and visualization, drill guide design and manufacturing. BMC oral health, 20(1), 251. https://doi.org/10.1186/s12903-020-01208-1

Kobayashi, K., Shimoda, S., Nakagawa, Y., & Yamamoto, A. (2004). Accuracy in measurement of distance using limited cone-beam computerized tomography. The International journal of oral & maxillofacial implants, 19(2), 228–231.

Luangchana, P., Pornprasertsuk-Damrongsri, S., Kiattavorncharoen, S., & Jirajariyavej, B. (2015). Accuracy of linear measurements using cone beam computed tomography and panoramic radiography in dental implant treatment planning. The International journal of oral & maxillofacial implants, 30(6), 1287–1294. https://doi.org/10.11607/jomi.4073

MacDonald, D. S., Colosi, D. C., Mupparapu, M., Kumar, V., Shintaku, W. H., & Ahmad, M. (2021). Guidelines for oral and maxillofacial imaging: COVID-19 considerations. Oral surgery, oral medicine, oral pathology and oral radiology, 131(1), 99–110. https://doi.org/10.1016/j.oooo.2020.10.017

MacDonald, D. (2020). Oral and maxillofacial radiology: A diagnostic approach (Second ed., pp 83-103). Hoboken, NJ: Wiley-Blackwell. doi: 10.1002/9781118786734

MacDonald, D. (2011). Oral and maxillofacial radiology: A diagnostic approach. (First ed., pp 59-60). Ames, Iowa; Chichester, West Sussex: Wiley-Blackwell Online Books, & Wiley Onlin Library. doi: 10.1002/9781119218739

Mandelaris, G.A., Scheyer, E.T., Evans, M., Kim, D., McAllister, B., Nevins, M.L., Rios, H.F. and Sarment, D. (2017), American Academy of Periodontology Best Evidence Consensus Statement on Selected Oral Applications for Cone-Beam Computed Tomography. Journal of Periodontology, 88: 939-945. https://doi.org/10.1902/jop.2017.170234

Menezes, C. C., Janson, G., da Silveira Massaro, C., Cambiaghi, L., & Garib, D. G. (2016). Precision, reproducibility, and accuracy of bone crest level measurements of CBCT cross sections using different resolutions. The Angle orthodontist, 86(4), 535–542. https://doi.org/10.2319/040115-214.1

Morton, DA, Foreman K, Albertine KH. The Big Picture: Gross Anatomy, 2e; 2019. Available at: https://accessmedicine.mhmedical.com/content.aspx?sectionid=202021212&bookid=2478 Accessed: July 05, 2020

Neiva, R.F., Gapski, R. and Wang, H.-L. (2004), Morphometric Analysis of Implant-Related Anatomy in Caucasian Skulls. Journal of Periodontology, 75: 1061-1067. https://doi.org/10.1902/jop.2004.75.8.1061

Neves, F. S., Vasconcelos, T. V., Campos, P. S., Haiter-Neto, F., & Freitas, D. Q. (2014). Influence of scan mode (180°/360°) of the cone beam computed tomography for preoperative dental implant measurements. Clinical oral implants research, 25(2), e155–e158. https://doi.org/10.1111/clr.12080

Newman, M. G., Takei, H., Klokkevold, P. R., & Carranza, F. A. (2011). Carranza's clinical periodontology. ProQuest Ebook Central https://ebookcentral.proquest.com

Patcas, R., Müller, L., Ullrich, O., & Peltomäki, T. (2012). Accuracy of cone-beam computed tomography at different resolutions assessed on the bony covering of the mandibular anterior teeth. American journal of orthodontics and dentofacial orthopedics, 141(1), 41–50. https://doi.org/10.1016/j.ajodo.2011.06.034

Pauwels, R., Araki, K., Siewerdsen, J. H., & Thongvigitmanee, S. S. (2015). Technical aspects of dental CBCT: state of the art. Dento maxillo facial radiology, 44(1), 20140224. https://doi.org/10.1259/dmfr.20140224

Phillips, J. L., Weller, R. N., & Kulild, J. C. (1990). The mental foramen: 1. Size, orientation, and positional relationship to the mandibular second premolar. Journal of endodontics, 16(5), 221–223. https://doi.org/10.1016/s0099-2399(06)81674-2

Radic, J., Patcas, R., Stadlinger, B., Wiedemeier, D., Rücker, M., & Giacomelli-Hiestand, B. (2018). Do we need CBCTs for sufficient diagnostics?-dentist-related factors. International journal of implant dentistry, 4(1), 37. https://doi.org/10.1186/s40729-018-0147-1

Schulze, R., Heil, U., Gross, D., Bruellmann, D. D., Dranischnikow, E., Schwanecke, U., & Schoemer, E. (2011). Artefacts in CBCT: a review. Dento maxillo facial radiology, 40(5), 265–273. https://doi.org/10.1259/dmfr/30642039

Sewerin I. P. (1990). Errors in radiographic assessment of marginal bone height around osseointegrated implants. Scandinavian journal of dental research, 98(5), 428–433. https://doi.org/10.1111/j.1600-0722.1990.tb00994.x

Sonick, M., Abrahams, J., & Faiella, R. (1997). A Comparison of the Accuracy of Periapical, Panoramic, and Computerized Tomographic Radiographs in Locating the Mandibular Canal. International journal of oral and maxillofacial implants, 9:455–460

Suomalainen, A., Vehmas, T., Kortesniemi, M., Robinson, S., & Peltola, J. (2008). Accuracy of linear measurements using dental cone beam and conventional multislice computed tomography. Dento maxillo facial radiology, 37(1), 10–17. https://doi.org/10.1259/dmfr/14140281

Sur, J., Seki, K., Koizumi, H., Nakajima, K., & Okano, T. (2010). Effects of tube current on cone-beam computerized tomography image quality for presurgical implant planning in vitro. Oral surgery, oral medicine, oral pathology, oral radiology, and endodontics, 110(3), e29–e33. https://doi.org/10.1016/j.tripleo.2010.03.041

Tahmaseb, A., Wismeijer, D., Coucke, W., & Derksen, W. (2014). Computer technology applications in surgical implant dentistry: a systematic review. The International journal of oral & maxillofacial implants, 29 Suppl, 25–42. https://doi.org/10.11607/jomi.2014suppl.g1.2

Torres, M. G., Campos, P. S., Segundo, N. P., Navarro, M., & Crusoé-Rebello, I. (2012). Accuracy of linear measurements in cone beam computed tomography with different voxel sizes. Implant dentistry, 21(2), 150–155. https://doi.org/10.1097/ID.0b013e31824bf93c

Vasconcelos, T.V., Neves, F.S., Moraes L.B., & Freitas, D.Q. (2015). Vertical bone measurements from cone beam computed tomography images using different software packages. Brazilian Oral Research, 29(1), 1-6. .https://dx.doi.org/10.1590/1807-3107BOR-2015.vol29.0035

Vercruyssen, M., Laleman, I., Jacobs, R., & Quirynen, M. (2015). Computer-supported implant planning and guided surgery: a narrative review. Clinical oral implants research, 26 Suppl 11, 69–76. https://doi.org/10.1111/clr.12638

Waltrick, K. B., Nunes de Abreu Junior, M. J., Corrêa, M., Zastrow, M. D., & Dutra, V. D. (2013). Accuracy of linear measurements and visibility of the mandibular canal of cone-beam computed tomography images with different voxel sizes: an in vitro study. Journal of periodontology, 84(1), 68–77. https://doi.org/10.1902/jop.2012.110524

Woelber, J. P., Fleiner, J., Rau, J., Ratka-Krüger, P., & Hannig, C. (2018). Accuracy and Usefulness of CBCT in Periodontology: A Systematic Review of the Literature. The International journal of periodontics & restorative dentistry, 38(2), 289–297. https://doi.org/10.11607/prd.2751

Yosue, T., & Brooks, S. L. (1989). The appearance of mental foramina on panoramic and periapical radiographs. II. Experimental evaluation. Oral surgery, oral medicine, and oral pathology, 68(4), 488–492. https://doi.org/10.1016/0030-4220(89)90151-5

Appendices

Appendix A

A.1 Data tables Mandible 1 – First reading and second reading

Table 21 and 22 represents the measured distances in each software with the corresponding scanning parameters. Scanning parameters are represented by mA, kvP and voxel sizes. Each measured distance also corresponds to its location. “Vol. #” represents the each scanned file saved under a specific volume set. Table 21 and 22 represent the first and second reading of the same volume set .

Software	Vol #	mA	kvP	Voxel	RM2	RM1	RP2	RC	I	LC	LP2	LM1	LM2
DTX	Vol. 20	3.2	90	180	22.5	23.2	16.9	36.4	35.2	36.8	17.8	24	22.3
	Vol. 23	4	90	180	22.5	23	16.9	36.8	35	36.2	17.4	23.4	22.4
	Vol. 24	5	90	180	23.7	23.2	16.7	37	34.9	37	17.8	24.3	22.5
	Vol. 25	3.2	90	300	22.6	22.5	16.2	35.8	35.9	37.1	16.8	23.9	22.5
	Vol. 26	4	90	300	22.1	22.6	17.3	36.8	35.3	36.5	17.4	24	24
	Vol. 27	5	90	300	22	23.3	16	35.3	34.6	37.2	17.6	23.3	22.9
					RM2	RM1	RP2	RC	I	LC	LP2	LM1	LM2
coDiagnostix	Vol. 20	3.2	90	180	22.2	22	16.7	37	36.5	36.3	17	22.6	22.2
	Vol. 23	4	90	180	22.7	21.8	16.1	34.7	35.6	36.1	17.4	22.5	22.8
	Vol. 24	5	90	180	22.8	21.4	16.5	35.4	36.2	36.2	17.4	22.8	22.9
	Vol. 25	3.2	90	300	22.8	21.3	16.9	34.9	35.3	36.7	17.7	23.3	22.4
	Vol. 26	4	90	300	22.2	23	16.3	35.6	36.1	35.9	17.4	23.2	22.5
	Vol. 27	5	90	300	23.2	21.7	16.6	34.3	35.4	35	17.2	23.4	23.8
					RM2	RM1	RP2	RC	I	LC	LP2	LM1	LM2
BlueSky Plan	Vol. 20	3.2	90	180	22.1	22.13	16.43	35.17	34.78	36.67	16.23	23.43	22.8
	Vol. 23	4	90	180	22.54	22.77	15.36	34.75	35.18	35.79	16.67	23.56	21.77
	Vol. 24	5	90	180	22.83	23.03	15.84	34.49	34.04	35.6	16.24	23.35	22.36
	Vol. 25	3.2	90	300	21.25	22.4	15.25	34.55	35.24	35.62	17.25	23.43	22.81
	Vol. 26	4	90	300	22.5	22.69	15.94	34.89	35.29	34.93	16.75	23.59	22.17
	Vol. 27	5	90	300	21.97	22.68	15.12	34.92	35.34	35.42	16.76	23.38	22.36
					RM2	RM1	RP2	RC	I	LC	LP2	LM1	LM2
Simplant	Vol. 20	3.2	90	180	22.05	21.7	16.02	35.69	35.67	35.98	16.89	22.62	22.16
	Vol. 23	4	90	180	20.67	22.18	14.98	36.29	35.5	36.48	16.71	23.04	22.93
	Vol. 24	5	90	180	21.64	21.95	15.38	35.72	35.15	36.83	16.32	23.12	22.03
	Vol. 25	3.2	90	300	21.43	22.34	16.29	35.36	35.54	37.02	17.12	23.17	22.52
	Vol. 26	4	90	300	21.83	22.6	15.78	35.89	35.28	36.66	17.25	23.73	22.7
	Vol. 27	5	90	300	22.26	23.06	15.95	35.19	34.57	36.48	16.76	22.92	23.58

Table 21: Measured distance (in mm) corresponding to each scanned parameter and location in each of the four softwares

Software	Scan #	mA	kvP	Voxel	RM2	RM1	RP2	RC	I	LC	LP2	LM1	LM2
DTX	Vol. 20	3.2	90	180	22.5	22.4	14.8	37.2	35.7	35.6	15.9	23.5	22.5
	Vol. 23	4	90	180	22.4	22.5	15.3	37.5	35.6	37.1	15.8	23.8	22.8
	Vol. 24	5	90	180	22.6	22.7	15.2	37.1	35.3	36.6	16.5	23.4	22.9
	Vol. 25	3.2	90	300	22.5	23.3	15.5	36.4	35.1	36.5	16.4	24.3	23
	Vol. 26	4	90	300	22	22.6	14.7	37.2	35.4	36.5	16.9	22.7	22.9
	Vol. 27	5	90	300	22	22.7	15.1	36.9	34.7	36.9	16.8	23.2	23.2
					RM2	RM1	RP2	RC	I	LC	LP2	LM1	LM2
coDiagnostix	Vol. 20	3.2	90	180	22.1	23	16.4	36.5	36.2	36.3	16.5	23.7	22.6
	Vol. 23	4	90	180	22.3	22.3	16	36.3	35.7	36.3	16.9	23.5	22.3
	Vol. 24	5	90	180	21.7	22.4	16.3	36.1	35.6	37.1	17.3	24	23
	Vol. 25	3.2	90	300	22.3	22	15.7	36.8	36.3	36.8	17.3	24.2	22.2
	Vol. 26	4	90	300	21.7	21.4	16.6	36.4	35.9	37.2	17.6	23.3	21.5
	Vol. 27	5	90	300	21.7	22.5	17	36.1	34.5	36.6	17	23.5	22.9
					RM2	RM1	RP2	RC	I	LC	LP2	LM1	LM2
BlueSky Plan	Vol. 20	3.2	90	180	21.99	23.2	16	35.82	34.15	35.46	16.31	23.21	21.86
	Vol. 23	4	90	180	21.54	23.27	16.27	36.13	34.14	36.85	16.04	22.83	22.2
	Vol. 24	5	90	180	21.8	21.75	15.91	36.84	34.73	36.33	16.86	23.11	22.83
	Vol. 25	3.2	90	300	22.08	22.15	15.72	36.39	35.6	35.35	15.89	23.49	21.94
	Vol. 26	4	90	300	22.07	22.14	15.63	36.04	34.21	36.5	16.64	22.93	22.46
	Vol. 27	5	90	300	21	22.64	15.9	35.55	33.74	36.52	16.6	22.84	23.07
					RM2	RM1	RP2	RC	I	LC	LP2	LM1	LM2
Simplant	Vol. 20	3.2	90	180	22.28	22.27	15.72	36.61	35.98	35.85	17.22	23.94	22.85
	Vol. 23	4	90	180	22.64	22.25	15.73	35.95	35.98	37.28	17.89	23.76	22.55
	Vol. 24	5	90	180	21.09	22.47	16.42	36.91	36.4	37.07	17.36	24.05	22.24
	Vol. 25	3.2	90	300	22.53	22.05	17.05	35.52	35.67	37.65	17.69	24.23	22.51
	Vol. 26	4	90	300	22.55	22.16	16.64	36.29	35.98	37.58	17.03	23.06	22.47
	Vol. 27	5	90	300	21.23	22.25	16.02	35.81	35.6	37.11	17.42	23.22	22.4

Table 22: Measured distance (in mm) corresponding to each scanned parameter and location in each of the four softwares

A.2 Data tables Mandible 2 – First and Second reading

Table 23 and 24 represents the measured distances in each software with the corresponding scanning parameters. Scanning parameters are represented by mA, kvP and voxel sizes. Each measured distance also corresponds to its location. “Vol. #” represents the each scanned file saved under a specific volume set. Table 23 and 24 represent the first and second reading of the same volume set.

Software	Scan #	mA	kvP	Voxel	RM2	RM1	RP2	RP1	RC	LC	LP1	LP2	LM1	LM2
DTX	Vol. 8	3.2	90	180	14.2	13.5	14.1	12.7	24.9	28.6	10.1	14.7	14.3	12.9
	Vol. 9	4	90	180	13.6	13.9	13.7	12.2	25.2	28.5	9.5	14.6	14.1	13.5
	Vol. 10	5	90	180	14	14.3	13.5	12.3	25.9	28.3	9.8	13.5	13.3	12.9
	Vol. 11	3.2	90	300	14.2	14.2	14.4	12	25.6	28.6	9.7	14.7	13.7	12.9
	Vol. 12	4	90	300	14	13.5	14.1	12.5	25.7	28.4	10.1	14.5	13.7	12.4
	Vol. 13	5	90	300	14.3	13.9	13.5	12.3	25.8	28	10.1	14	14.1	13.5
					RM2	RM1	RP2	RP1	RC	LC	LP1	LP2	LM1	LM2
coDiagnostix	Vol. 8	3.2	90	180	12.9	13.2	13.9	13.4	25.9	28.4	10.1	13.5	13.9	13.2
	Vol. 9	4	90	180	13.3	13.6	13	13.7	25.2	28.3	10.4	14.1	14.1	13.2
	Vol. 10	5	90	180	13	13.3	13.8	12.2	25.6	28.4	10	13.9	13.6	13.6
	Vol. 11	3.2	90	300	13.6	13.5	14	13.3	25.3	28.5	9.9	13.9	12.9	13.7
	Vol. 12	4	90	300	13.9	13.3	13.3	13.2	26	28.4	9.5	13.9	13.4	12.8
	Vol. 13	5	90	300	13.7	13.8	13.6	12.8	25.9	28.3	9.8	14	13.2	13.3
					RM2	RM1	RP2	RP1	RC	LC	LP1	LP2	LM1	LM2
BlueSky Plan	Vol. 8	3.2	90	180	13.62	13.38	13.86	13.67	25.84	27.74	10.36	14.61	14.31	13.81
	Vol. 9	4	90	180	12.2	12.82	13.82	13.23	24.99	27.13	9	14.95	14.32	13.54
	Vol. 10	5	90	180	13.52	13.57	13.71	12.9	25.35	27.46	9.49	14.18	14.18	12.81
	Vol. 11	3.2	90	300	13.03	13.02	14	13.46	25.94	27.91	9.41	14.34	14.01	13.33
	Vol. 12	4	90	300	13.14	13.76	14.32	13.37	25.95	27.82	8.97	14.61	14.05	13.65
	Vol. 13	5	90	300	13.77	12.91	13.19	12.99	25.4	27.49	9.09	14.52	14.74	13.67
					RM2	RM1	RP2	RP1	RC	LC	LP1	LP2	LM1	LM2
Simplant	Vol. 8	3.2	90	180	12.79	13.5	13.83	12.43	26.21	28.27	10.29	13.83	13.12	12.21
	Vol. 9	4	90	180	13.22	12.41	13.47	12.69	25.88	27.5	10.15	13.3	13.39	13.75
	Vol. 10	5	90	180	13.03	13.47	13.65	12.09	25.75	27.88	9.4	13.85	12.99	13.53
	Vol. 11	3.2	90	300	12.96	13.15	13.83	12.09	25.81	28.24	9.71	14.25	13.57	13.41
	Vol. 12	4	90	300	12.7	13.75	13.29	12.03	26.43	28.28	9.1	14.59	13.7	13.57
	Vol. 13	5	90	300	12.51	13.37	13.66	12.58	26.42	28.59	10.33	13.66	12.99	12.43

Table 23: Measured distance (in mm) corresponding to each scanned parameter and location in each of the four software

Software	Scan #	mA	kvP	Voxel	RM2	RM1	RP2	RP1	RC	LC	LP1	LP2	LM1	LM2
DTX	Vol. 8	3.2	90	180	13.1	13.2	13.9	12.5	25.6	27.9	9.5	14.3	13.8	13.8
	Vol. 9	4	90	180	12.9	13	13.6	12.2	26	28.2	9.8	14.4	13.9	14
	Vol. 10	5	90	180	13.6	12.8	13.2	12.1	26.2	27.8	9.3	14.1	13.2	12.9
	Vol. 11	3.2	90	300	13.8	13.1	13.7	12.1	26.1	28.8	9.8	14.2	13.7	12.9
	Vol. 12	4	90	300	12.5	13.5	13.7	12.1	25.9	28.3	9.6	13.9	12.9	13.3
	Vol. 13	5	90	300	13.4	12.5	13.4	12.5	26.2	28.3	9.8	13.6	13	13.7
					RM2	RM1	RP2	RP1	RC	LC	LP1	LP2	LM1	LM2
coDiagnostix	Vol. 8	3.2	90	180	13.5	13.3	13.7	13.6	25.7	28.6	10	14.3	13.4	13.5
	Vol. 9	4	90	180	13.2	13.9	14.1	13.1	26.1	28	9.8	14.8	14	12.6
	Vol. 10	5	90	180	13.9	13	14.1	13.1	25.6	28.2	10	15.1	13.8	13.2
	Vol. 11	3.2	90	300	13.1	14.5	13.8	13.1	26.3	28.3	10.3	14.6	14.3	13
	Vol. 12	4	90	300	13.8	13.2	13.7	13	26.1	28.2	10.4	15.2	14.5	13.3
	Vol. 13	5	90	300	13.6	13.5	14.5	12.8	25.5	28.8	9.9	14.7	13.3	13.2
					RM2	RM1	RP2	RP1	RC	LC	LP1	LP2	LM1	LM2
BlueSky Plan	Vol. 8	3.2	90	180	13.25	13.13	13.3	13.62	25.25	27.91	9.47	15.05	13.82	12.6
	Vol. 9	4	90	180	13.01	13.3	13.13	12.88	25.31	27.05	9.27	14.53	13.48	13.82
	Vol. 10	5	90	180	13.32	12.94	13.73	12.54	25.29	27.11	10.2	13.91	13.45	13.15
	Vol. 11	3.2	90	300	13.05	13.26	13.55	13.28	25.85	27.89	9.44	14.2	13.71	12.43
	Vol. 12	4	90	300	13.43	13.55	14.03	12.36	25.61	26.8	9.7	14.58	14.57	12.79
	Vol. 13	5	90	300	12.45	13.77	13.59	12.51	25.95	26.99	9.19	13.31	13.32	13.75
					RM2	RM1	RP2	RP1	RC	LC	LP1	LP2	LM1	LM2
Simplant	Vol. 8	3.2	90	180	13.11	13.63	13.31	12.38	25.9	28.18	10.08	14.32	13.5	11.3
	Vol. 9	4	90	180	12.43	13.77	13.56	13.46	25.9	27.93	9.93	13.83	13.46	12.22
	Vol. 10	5	90	180	13.1	13.4	13.7	12.98	25.98	28.62	9.72	13.46	13.12	12.71
	Vol. 11	3.2	90	300	13.16	13.23	13.44	13.28	26.22	28.18	10.57	13.98	13.34	12.9
	Vol. 12	4	90	300	13.71	13.21	13.81	13.18	25.59	28.55	9.93	13.57	13.21	12.93
	Vol. 13	5	90	300	13.6	12.98	13.56	12.42	25.93	28.67	9.54	13.57	13.38	13.29

Table 24: Measured distance (in mm) corresponding to each scanned parameter and location in each of the four software

A.3 Caliper / "Gold standard" measurements

Table 25 and 26 represents the caliper readings in millimeter for Mandible 1 and Mandible 2, respectively corresponding to the particular sections of interest.

Mandible 1	
Location	Distance (in mm)
RM2	21.23
RM1	22.54
RP2	16.5
RC	36.68
I	35.19
LC	35.1
LP2	17.28
LM1	23.29
LM2	22.78

Table 25: Distance measured (in mm) using digital calipers corresponding with the particular sections of interest in Mandible 1

Mandible 2	
Location	Distance (in mm)
RM2	13.73
RM1	13.22
RP2	13.72
RP1	12.58
RC	26.51
LC	28.12
LP1	10.32
LP2	13.91
LM1	14.36
LM2	13.12

Table 26: Distance measured (in mm) using digital calipers corresponding with the particular sections of interest in Mandible 2

Appendix B

Calculation of ICC:

Intra-correlation coefficient is also analyzed using the following formula which yielded a value of 0.988

```
> anova(lm(observed~id+reading,data2),data2)
Analysis of Variance Table

Response: observed
           Df Sum Sq Mean Sq  F value Pr(>F)
id          1  31362 31361.7 890.8307 <2e-16 ***
reading     1      0     0.0   0.0003 0.9851
Residuals 909  32001    35.2
---
Signif. codes:  0 ‘***’ 0.001 ‘**’ 0.01 ‘*’ 0.05 ‘.’ 0.1 ‘ ’ 1
```

$$ICC\ 1,1 = \frac{MS_B - MS_W}{MS_B + (k-1)MS_W} \qquad (4)$$

$MS_W = \frac{0+32001}{1+909} = 35.16593.$

$ICC = \frac{31361.7-35.16593}{31361.7+(2-1)35.16593} = 0.988$

Appendix C

Tables from Statistical Analysis

Table Analyzed	Mean error values MD1 / Caliper-Software					
Data sets analyzed	A-E					
ANOVA summary						
F	0.005066					
P value	>0.9999					
P value summary	ns					
Significant diff. among means (P < 0.05)	No					
R squared	0.0005064					
Brown-Forsythe test						
F (DFn, DFd)	0.002205 (4, 40)					
P value	>0.9999					
P value summary	ns					
Are SDs significantly different (P < 0.05)	No					
Bartlett's test						
Bartlett's statistic (corrected)	0.01765					
P value	>0.9999					
P value summary	ns					
Are SDs significantly different (P < 0.05)	No					
ANOVA table	**SS**		**DF**	**MS**	**F (DFn, DFd)**	**P value**
Treatment (between columns)	1.312		4	0.3281	F (4, 40) = 0.005066	P>0.9999
Residual (within columns)	2590		40	64.76		
Total	2592		44			
Data summary						
Number of treatments (columns)	5					
Number of values (total)	45					

Dunnett's multiple comparisons test	**95.00% CI of diff.**	**Below threshold?**	**Summary**	**Adjusted P Value**	**A-?**	
Caliper vs. DTX	-9.932 to 9.361	No	ns	0.9999	B	DTX
Caliper vs. CoD	-9.797 to 9.497	No	ns	>0.9999	C	CoD
Caliper vs. BSP	-9.423 to 9.870	No	ns	>0.9999	D	BSP
Caliper vs. SM	-9.761 to 9.532	No	ns	>0.9999	E	SM

Test details	**Mean 2**	**Mean Diff.**	**SE of diff.**	**n1**	**n2**	**q**	**DF**
Caliper vs. DTX	25.91	-0.2854	3.793	9	9	0.07523	40
Caliper vs. CoD	25.77	-0.1502	3.793	9	9	0.03959	40
Caliper vs. BSP	25.40	0.2236	3.793	9	9	0.05895	40
Caliper vs. SM	25.74	-0.1146	3.793	9	9	0.03022	40

Table 27: Caliper vs softwares – ANOVA analysis on mean values in Mandible 1

Table Analyzed	Mean error values MD2/ Caliper-Software					
Data sets analyzed	A-E					
ANOVA summary						
F	0.004108					
P value	>0.9999					
P value summary	ns					
Significant diff. among means (P < 0.05)'	No					
R squared	0.0003650					
Brown-Forsythe test						
F (DFn, DFd)	0.0005396 (4, 45)					
P value	>0.9999					
P value summary	ns					
Are SDs significantly different (P < 0.05)'	No					
Bartlett's test						
Bartlett's statistic (corrected)	0.02650					
P value	>0.9999					
P value summary	ns					
Are SDs significantly different (P < 0.05)'	No					
ANOVA table	**SS**		**DF**	**MS**	**F (DFn, DFd)**	**P value**
Treatment (between columns)	0.5996		4	0.1499	F (4, 45) = 0.004108	P>0.9999
Residual (within columns)	1642		45	36.49		
Total	1643		49			
Data summary						
Number of treatments (columns)	5					
Number of values (total)	50					

Dunnett's multiple comparisons test	**Mean Diff.**	**95.00% CI of diff.**	**Below threshold?**	**Summary**	**Adjusted P Value**	**A-?**		
Caliper vs. DTX	0.1582	-6.681 to 6.997	No	ns	>0.9999	B	DTX	
Caliper vs. coD	0.03317	-6.806 to 6.872	No	ns	>0.9999	C	coD	
Caliper vs. BSP	0.2260	-6.613 to 7.065	No	ns	0.9999	D	BSP	
Caliper vs. SM	0.2857	-6.553 to 7.124	No	ns	0.9999	E	SM	
Test details	**Mean 1**	**Mean 2**	**Mean Diff.**	**SE of diff.**	**n1**	**n2**	**q**	**DF**
Caliper vs. DTX	15.96	15.80	0.1582	2.701	10	10	0.05855	45
Caliper vs. coD	15.96	15.93	0.03317	2.701	10	10	0.01228	45
Caliper vs. BSP	15.96	15.73	0.2260	2.701	10	10	0.08366	45
Caliper vs. SM	15.96	15.67	0.2857	2.701	10	10	0.1057	45

Table 28: Caliper vs softwares – ANOVA analysis on mean values in Mandible 2

Appendix D

Table Analyzed	MD 1 - master				
Two-way RM ANOVA	Matching: Stacked				
Assume sphericity?	No				
Alpha	0.05				
Source of Variation	**% of total variation**	**P value**	**P value summary**	**Significant?**	**Geisser-Greenhouse's**
Location x Different Softwares	0.2479	0.4027	ns	No	
Location	99.39	<0.0001	****	Yes	0.6177
Different Softwares	0.06974	0.0919	ns	No	
Subject	0.04217	0.1309	ns	No	
ANOVA table	**SS**	**DF**	**MS**	**F (DFn, DFd)**	**P value**
Location x Different Softwares	65.01	192	0.3386	F (192, 200) = 1.036	P=0.4027
Location	26064	8	3258	F (4.942, 123.5) = 9966	P<0.0001
Different Softwares	18.29	24	0.7620	F (24, 25) = 1.723	P=0.0919
Subject	11.06	25	0.4423	F (25, 200) = 1.353	P=0.1309
Residual	65.39	200	0.3269		
Data summary					
Number of columns (Different Softwares	25				
Number of rows (Location)	9				
Number of subjects (Subject)	50				
Number of missing values	0				

Table 29: Location vs Different Softwares – Two-way ANOVA analysis in Mandible 1

Dunnett's multiple comparison test was carried out all of the scanned parameters at each location, only significant findings are listed below.

Dunnett's multiple comparisons test	Mean Diff.	95.00% CI of diff.	Below threshold?	Summary	Adjusted P Value
RM2					
Caliper vs. 3.2mA 180Voxel DTX	-1.27		Yes	***	0.0001
Caliper vs. 5mA 300Voxel DTX	-0.77		Yes	***	0.0001
RM1					
Caliper vs. 4mA 300Voxel DTX	-0.06		Yes	***	0.0001
LC					
Caliper vs. 4mA 300Voxel DTX	-1.4		Yes	***	0.0001
Caliper vs. 3.2mA 180Voxel coD	-1.2		Yes	***	0.0001
Caliper vs. 3.2mA 300Voxel coD	-1.65	-3.224 to -0.07579	Yes	*	0.0478
LM2					

Caliper vs. 3.2mA 300Voxel SP	0.265	0.1076 to 0.4224	Yes	*	0.0295

Table 30: Location vs Different softwares – Dunnett's multiple comparison test in Mandible 1

Table Analyzed	MD 2 - ALL				
Two-way RM ANOVA	Matching: Stacked				
Assume sphericity?	No				
Alpha	0.05				
Source of Variation	**% of total variation**	**P value**	**P value summary**	**Significant?**	**Geisser-Greenhous**
Location x Different Software	0.3058	0.0046	**	Yes	
Location	99.39	<0.0001	****	Yes	0.6433
Different Software	0.05086	0.1114	ns	No	
Subject	0.03219	0.1669	ns	No	
ANOVA table	**SS**	**DF**	**MS**	**F (DFn, DFd)**	**P value**
Location x Different Software	50.26	216	0.2327	F (216, 225) = 1.421	P=0.0046
Location	16334	9	1815	F (5.790, 144.7) = 11084	P<0.0001
Different Software	8.358	24	0.3483	F (24, 25) = 1.646	P=0.1114
Subject	5.290	25	0.2116	F (25, 225) = 1.292	P=0.1669
Residual	36.84	225	0.1637		
Data summary					
Number of columns (Different Software	25				
Number of rows (Location)	10				
Number of subjects (Subject)	50				
Number of missing values	0				

Table 31: Location vs Different Softwares – Two-way ANOVA analysis in Mandible 2

Dunnett's multiple comparison test was carried out all of the scanned parameters at each location, only statistically significant findings are listed below.

Dunnett's multiple comparisons test	Mean Diff.	95.00% CI of diff.	Below threshold?	Summary	Adjusted P Value
RM2					
Caliper vs. 3.2mA 300Voxel BSP	0.69	0.3752 to 1.005	Yes	*	0.0224
RM1					
Caliper vs. 4mA 300Voxel DTX	-0.28		Yes	***	0.0001
RP1					
Caliper vs. 4mA 180Voxel DTX	0.38		Yes	***	0.0001
Caliper vs. 5mA 300Voxel coD	-0.22		Yes	***	0.0001
Caliper vs. 3.2mA 180Voxel BSP	-1.065	-1.852 to -0.2779	Yes	*	0.0374
RC					
Caliper vs. 5mA 180Voxel coD	0.91		Yes	***	0.0001

Caliper vs. 5mA 180Voxel BSP	1.19	0.2455 to 2.135	Yes	*	0.0401
Caliper vs. 4mA 180Voxel SM	0.62	0.3052 to 0.9348	Yes	*	0.0248
LP1					
Caliper vs. 5mA 180Voxel coD	0.32		Yes	***	0.0001
Caliper vs. 3.2mA 300Voxel BSP	0.895	0.4227 to 1.367	Yes	*	0.0258
LP2					
Caliper vs. 4mA 300Voxel BSP	-0.685	-1.157 to -0.2127	Yes	*	0.0347
LM1					
Caliper vs. 3.2mA 300Voxel DTX	0.66		Yes	***	0.0001
LM2					
Caliper vs. 5mA 180Voxel DTX	0.22		Yes	***	0.0001
Caliper vs. 3.2mA 300Voxel DTX	0.22		Yes	***	0.0001

Table 32: Location vs Different softwares – Dunnett's multiple comparison test in Mandible 2

Calculation of Average mean difference between BSP and coD

(Avg. mean difference from caliper vs. BSP – Avg. mean difference from caliper vs coD) X difference in accuracy : values derived from Table 16

= 0.15 – (-0.22) x 0.006 = 0.002mm

Appendix E

Paired t test Tabular results	
Table Analyzed	MD1 vs MD2
Column B	MD2
vs.	vs.
Column A	MD1
Paired t test	
P value	0.0865
P value summary	ns
Significantly different (P < 0.05)?	No
One- or two-tailed P value?	Two-tailed
t, df	t=2.516, df=3
Number of pairs	4
How big is the difference?	
Mean of differences (B - A)	0.2574
SD of differences	0.2046
SEM of differences	0.1023
95% confidence interval	-0.06816 to 0.5830
R squared (partial eta squared)	0.6785
How effective was the pairing?	
Correlation coefficient (r)	0.3562
P value (one tailed)	0.3219
P value summary	ns
Was the pairing significantly effective?	No

Figure 31: Paired t-test to compare mean differences between MD1 and MD2